03

Volumetric integro-differential equations in diffraction and eigenvalue problems (review)

© M.V. Davidovich

Saratov National Research State University,
410012 Saratov, Russia

e-mail: Davidovichmv@info.sgu.ru

Received February 5, 2022
Revised June 26, 2022
Accepted July 4, 2022

Volumetric integral and integro-differential equations are considered that describe problems of diffraction by three-dimensional bodies with given macroscopic permittivity and magnetic permeability, as well as problems on free vibrations of such bodies. Similar equations are obtained for waveguide structures: hollow shielded waveguides with dielectric filling, dielectric waveguides (optical beamguides), photonic-crystal waveguides. Dominantly stationary linear electromagnetic problems are considered. Non-stationary and nonlinear problems are mentioned casually. Numerical results are given for oscillations $H_{01\delta}$ and H_{011} of a cylindrical dielectric resonator, for waves of a rectangular dielectric waveguide and a plasmonic waveguide, dispersion in a photonic crystal, and diffraction by a rectangular dielectric cylinder.

Keywords: ...

DOI: 10.21883/EOS.2022.10.54863.3231-22

1. Introduction

Volumetric integral equations (VIEs) are based on the representation of fields inside the volumes of bodies. They were mainly used for structures with dielectric inclusions in problems of electrodynamics and optics [1–27]. For the first time, apparently, they were introduced in the work [1]. The principle of obtaining them is very simple: any body that has an electrical and/or magnetic response to the action of the field is described by its polarization currents as if they are located in a vacuum in the volume occupied by the body [28]. This makes it possible to use the apparatus of vacuum tensor Green's functions (FGs) to formulate the VIE, which are clearly known for free space [28] and for some simple shielded regions with electric and magnetic walls: hollow rectangular and round cylindrical waveguides and resonators, spherical resonator and a number of others. Dielectric bodies in vacuum and in the indicated structures are described by VIEs. The use of impedance screens complicates the problems, leading to combined volume-surface integral equations (IE), which we do not consider in detail here. Since metals are well described by the dielectric permittivity (DP) of the Drude-Lorentz model $\varepsilon_m(\omega, \mathbf{r}) = \varepsilon_L(\omega, \mathbf{r}) - \omega_p^2/(\omega^2 - i\omega\omega_c)$, in which the Lorentz term ε_L is almost constant and real up to the plasma frequency ω_p, then the VIE describe small metallic particles and plasmons in them, including localized plasmons. To describe a field in a metal, one or all dimensions must be comparable with the penetration depth, otherwise the metal body should be considered as an impedance surface with a given surface impedance. Recently, electrodynamic and optical problems have arisen for bodies made of metamaterials with effective (obtained by homogenization) material parameters [16–18,29]. Such metamaterials can be chiral, biisotropic and bianisotropic with electric and magnetic responses. In the frequency region where the homogenization is performed correctly and the spatial dispersion can be neglected, bodies made of metamaterials can also be compared with the VIE in the frequency domain. Note that the bodies of their photonic crystals (PCs) in optics can in principle be described only by a tensor DP with allowance for spatial dispersion. Then the use of the VIE is possible only in the frequency region where the spatial dispersion can be neglected Finally, VIE can be formulated in the space-time domain [14,23]. Such non-stationary VIEs have recently become more and more widely used. The specified wide range of possible applications of VIE is not sufficiently reflected in publications, which mainly consider the problems of diffraction by dielectric bodies. One of the objectives of the review is to reveal the possibilities of the VIE method.

Although by now a significant number of commercial software packages have appeared based on finite-difference (grid) methods in the space-frequency (FDFD) and space-time domains (FDTD), projection methods such as the method of moments (MoM), variational methods such as the method of finite elements (FEM) and a number of other approaches to solving Maxwell's equations, which make it possible to analyze the structures considered in the review, VIEs find more and more applications in electrodynamics, optics, and other areas. The advantages of VIE are especially evident for open boundary value problems and similar problems with infinitely distant

boundaries, for inhomogeneous, nonlinear, anisotropic and bianisotropic structures, where it is not very convenient or even impossible to work with commercial packages. Especially the advantages of VIE are manifested for bodies of small electrical dimensions (the electrical size of a body is determined by the number of wavelengths inside it). This, for example, is typical for localized plasmons in metal nanoparticles, for plasmonic and magnetoplasmonic waveguides. An example of the advantage of modeling by the VIE method can be a sparse PC from dielectric inclusions, when the area of inclusions is small compared to the entire area — of the periodicity cell. If a PC consists of a dielectric base into which objects (meta-atoms) are periodically embedded, then to model the dispersion, one should use the GF of an unlimited space with the DP of the base For open problems, the area inside the bodies is usually finite, and the solution area is infinite, which creates difficulties for a number of methods, for example, the grid method or the finite difference method (FDM), FEM. For such problems, the VIE method gives solutions with the fulfillment of the radiation condition, i.e., correctly represents fields in the far-field region. The solution of VIE based on discretization using volumetric finite elements (FE) allows reducing the mathematical dimension of problems by orders of magnitude (the number of nodes, the number of FE or basis functions) in comparison with grid methods and FE-type methods based on Maxwell's differential equations. Below, the dimension of the problem will be understood as the dimension of the matrix during discretization. True, FDM and FEM lead to sparse matrices, while FEM gives everywhere dense matrices. But this is a small price to pay for its advantages, especially since such problems are usually solved iteratively. In principle, the approach based on the VIE method using volumetric FEs makes it possible to implement fairly universal software systems, but this, apparently, is the area of future implementations of commercial electrodynamic simulation software packages. Similar work is being done. The convenience of the VIE method is also the fact that on its basis bilinear and quadratic functionals are easily formulated, the determination of the stationary values of which makes it possible to determine the fields or integral parameters of problems, for example, the frequencies of dielectric resonators (DR), reflection coefficients, scattering cross sections, direction response patterns. It is convenient to perform homogenization for PCs and metamaterials on the basis of the VIE solution [16–18], which is difficult to do using commercial packages.

In this review, we mainly consider three-dimensional open and screened boundary value problems with field penetration into the volume, which are formulated as diffraction problems or as eigenvalue problems. The two-dimensional problem of free waves of a waveguide is considered as a special case. Three-dimensional problems of wave diffraction on impedance and ideal surfaces (surface integral equations), as well as problems of diffraction on bulk and other inhomogeneities in waveguides are not considered and are mentioned in passing. Many methods have been developed for these problems, including the theory of waveguide excitation [28,30,31], especially in cases where the eigenwave spectrum is known. In the general case, we denote by the term VIE also volumetric integro-differential equations (IDEs). There is disagreement about the definition of which equations should be attributed to the IDE. Often, hypersingular IEs are referred to as IDEs, when the operator $\nabla \otimes \nabla = \mathrm{grad}(\mathrm{div})$ acts on the integral (i.e., on the kernel). We will call IDE equations in which both integral and differential operators act on the desired function, and the latter can act both on the function under the integral and on the non-integral term with it. The last case is reduced to the first by the formal introduction of the delta singularity into the kernel.

2. Integral and integro-differential equations

An arbitrary body of volume V bounded by a surface S in free space, described by a frequency macroscopic DP $\varepsilon(\omega, \mathbf{r})$, is equivalent to the action of the polarization electric current density $\mathbf{J}_\varepsilon^p(\omega, \mathbf{r}) = \partial_i \mathbf{P}_\varepsilon = i\omega\varepsilon_0(\varepsilon(\omega, \mathbf{r}) - 1)\mathbf{E}(\omega, \mathbf{r})$, where $\mathbf{E}(\omega, \mathbf{r})$ — field, satisfying Maxwell's equations. $\nabla\times\mathbf{H}(\omega, \mathbf{r}) = i\omega\varepsilon_0\mathbf{E}(\varepsilon(\omega, \mathbf{r}) + \mathbf{J}_\varepsilon^p(\omega, \mathbf{r}) + \mathbf{J}_0(\omega, \mathbf{r})$, where $\mathbf{J}_0(\omega, \mathbf{r})$ are third-party sources (density of third-party current) that create a field. Maxwell's second equation has a standard form. Sources should be introduced into it if the body has a response in the form of magnetic polarization. Next, we omit the word „density" and simply write „current". In the absence of a body, $\mathbf{J}_\varepsilon^p \equiv 0$, and $\mathbf{L}_0$ define a side field $\mathbf{E}_0$, bfH_0, which is convenient to add to the field excited by the body. In particular, when the sources are at infinity, this is a plane wave field. The body can be single-connected and multi-connected. If the body has magnetic properties, then the magnetic polarization current $\mathbf{L}_\mu^p(\omega, \mathbf{r}) = i\omega\mu_0$ is also added to another Maxwell equation $(\mu(\omega, \mathbf{r}) - 1)\mathbf{H}(\omega, \mathbf{r})$. The convenience of consideration lies in the fact that these sources are localized in the body, which can be inhomogeneous and anisotropic. If the body is anisotropic, then one should take the tensor values for the DP and magnetic permeability (MP):

$$\mathbf{J}_\varepsilon^p(\omega, \mathbf{r}) = i\omega\varepsilon_0(\hat{\varepsilon}(\omega, \mathbf{r}) - \hat{I})\mathbf{E}(\omega, \mathbf{r}),$$

$$\mathbf{J}_\mu^p(\omega, \mathbf{r}) = i\omega\mu_0(\hat{\mu}(\omega, \mathbf{r}) - \hat{I})\mathbf{H}(\omega, \mathbf{r}).$$

Further, everywhere $\hat{I}$ is the unit tensor. Moreover, one can consider a bianisotropic body. It take place the electrical polarization

$$\mathbf{P}_\varepsilon = \varepsilon_0\hat{\chi}_\varepsilon(\omega, \mathbf{r})\mathbf{E}(\omega, \mathbf{r}) + c^{-1}\hat{\xi}(\omega, \mathbf{r})\mathbf{H}(\omega, \mathbf{r})$$

and the magnetic polarization for it.

$$P_\mu = \mu_0\mathbf{M} = \mu_0\hat{\chi}_\mu(\omega, \mathbf{r})\mathbf{H}(\omega, \mathbf{r}) + c^{-1}\hat{\xi}(\omega, \mathbf{r})\mathbf{E}(\omega, \mathbf{r}).$$

Here $\mathbf{M}$ is the magnetization vector. Accordingly, the introduced polarization currents are expressed in terms of the susceptibilities.

$$\hat{\chi}_\varepsilon(\omega, \mathbf{r}) = \hat{\varepsilon}(\omega, \mathbf{r}) - \hat{I},\ \hat{\chi}_\mu(\omega, \mathbf{r}) = \hat{\mu}(\omega, \mathbf{r}) - \hat{I}$$

and additionally in terms of the cross-polarization tensors $\hat{\varepsilon}$ and $\hat{\xi}$ if bianisotropy takes place. Bi-anisotropy requires consideration of two IDEs, as well as a simple accounting for electrical and magnetic properties. Cross-polarization leads to additional terms that do not affect the idea of algorithmization. We will not consider it. Polarization field (solution of homogeneous equations), is written by us in the form

$$\mathbf{E}^p(\mathbf{r}) = ik_0 \int\limits_V \lfloor \hat{D}G(k, \mathbf{r} - \mathbf{r}')\hat{\chi}'^{\varepsilon}(\mathbf{r}')\mathbf{E}^p(\mathbf{r}') - \eta_0 \nabla \times G(k, \mathbf{r} - \mathbf{r}')\hat{\chi}^{\mu}(\mathbf{r}')\mathbf{H}^p(\mathbf{r}') \rfloor d^3r', \quad (1)$$

$$\mathbf{H}^p(\mathbf{r}) = ik_0 \int\limits_V \lfloor \hat{D}G(k, \mathbf{r} - \mathbf{r}')\hat{\chi}'^{\mu}(\mathbf{r}')\mathbf{H}^p(\mathbf{r}') + \eta_0^{-1} \nabla \times G(k, \mathbf{r} - \mathbf{r}')\hat{\chi}'^{\varepsilon}(\mathbf{r}')\mathbf{E}^p(\mathbf{r}') \rfloor d^3r', \quad (2)$$

Here the differential operators $\hat{D} = -i(\nabla \otimes \nabla + k^2\hat{I})/k$, $\nabla \otimes \nabla = \nabla\nabla$, matrix $\nabla \otimes \nabla$ has components $\partial_\alpha \partial_\beta$, $\alpha, \beta = x, y, z$, $k = k_0\ sqrt\tilde{\varepsilon}$, the scalar GF $G(k, \mathbf{r} - \mathbf{r}') = (4\pi R)^{-1} \exp(-ikR)$, $\hat{\chi}'^{\varepsilon} = \hat{\varepsilon}(\mathbf{r})/\tilde{\varepsilon} - \hat{I}$, $k_0 = \omega/c$, $R = \mathbf{r} - \mathbf{r}'$ is the distance between source and observation point. For inhomogeneous structures with the GF-boundaries are depend on these points separately. In the general case, we consider bodies in a homogeneous unbounded medium without dispersion (base) with DP $\tilde{\varepsilon}$. Therefore, instead of $\hat{\varepsilon}(\omega, \mathbf{r})$ one should take $\hat{\varepsilon}(\omega, \mathbf{r})/\tilde{\varepsilon}$. For bodies in vacuum $G \equiv G_0(k_0, \mathbf{r}) = |4\pi\mathbf{r}|^{-1} \exp(-ik_0|\mathbf{r}|)$. Equations (1), (2) describe homogeneous problems, for example, problems of free (natural) oscillations of the DR. For inhomogeneous problems (diffraction problems), the source fields should be added to these fields:

$$\mathbf{E}^0(\mathbf{r}) = \int\limits_{V_0} \hat{D}G(k, \mathbf{r} - \mathbf{r}')\mathbf{J}^0(\mathbf{r}')d^3r', \quad (3)$$

$$\mathbf{H}^0(\mathbf{r}) = \int\limits_{V_0} \nabla \times G(k, \mathbf{r} - \mathbf{r}')\mathbf{J}^0(\mathbf{r}')d^3r'. \quad (4)$$

Here V_0 is volume occupied by field sources. Point dipoles can be taken as the simplest sources. Sources at infinity create plane waves, and the problem of diffraction of plane waves on a body arises. Now full fields are superpositions

$$\mathbf{E}(\mathbf{r}) = \mathbf{E}^0(\mathbf{r}) + \mathbf{E}^p(\mathbf{r}) = \mathbf{E}^0(\mathbf{r}) + \hat{K}_\varepsilon(\mathbf{r}, \mathbf{E}, \mathbf{H}), \quad (5)$$

$$\mathbf{H}(\mathbf{r}) = \mathbf{H}^0(\mathbf{r}) + \mathbf{H}^p(\mathbf{r}) = \mathbf{H}^0(\mathbf{r}) + \hat{K}_\mu(\mathbf{r}, \mathbf{E}, \mathbf{H}), \quad (6)$$

where the upper circumflexes denote integral operators. It is these total fields that should be used to calculate the polarization currents, i.e., to substitute for integrals.

Equations (5), (6) belong to singular equations of the Lippmann-Schwinger type [32]. In the original formulation (1), (2) their kernels have non-integrable singularities of the type $|\mathbf{r} - \mathbf{r}'|^{-3}$, which makes it impossible to use piecewise constant functions (or simple quadrature formulas) for their direct numerical solution. Often such IEs are called as hypersingular. Integrals of type (1), (2) diverge in the usual sense, so special spaces of basis and weight functions should be used, and the result should be understood in a generalized sense as a distribution (generalized function) [33–37]. Integrals diverging in the usual sense in such singular IEs should be understood in the Cauchy principal value sense [38,39], and their divergence in the usual sense is due to the fact that the corresponding integral operator, although bounded, is not completely continuous hbox[8,35–39]. Physically, the singularity is related to the GF of a point source, which has the singularity $|\mathbf{r} - \mathbf{r}'|^{-1}$. Its double differentiation in defining the fields leads to the maximum singularity $|\mathbf{r} - \mathbf{r}'|^{-3}$. To avoid such differentiation, it is convenient to reformulate the equations, in particular, to formulate the VIE for electrodynamic potentials [40]. They can be entered in different ways. Let?s demonstrate an example of such a formulation for dielectric body using an electric potential vector. It is defined by the equation

$$\mathbf{A}(\omega, \mathbf{r}) = \int\limits_V G(\mathbf{r} - \mathbf{r}')\mathbf{J}_p(\mathbf{r}')d^3r'.$$

Using the body polarization current $\mathbf{J}_p(\mathbf{r}) = i\omega\varepsilon_0(\varepsilon(\omega, \mathbf{r}) - 1)\mathbf{E}(\omega, \mathbf{r})$ and the expression of the electric field in terms of the electric vector-potential [28] $\mathbf{E}(\omega, \mathbf{r}) = \lfloor \nabla(\nabla \cdot \mathbf{A}(\omega, \mathbf{r})) + k_0^2\mathbf{A}(\omega, \mathbf{r}) \rfloor / (i\omega\varepsilon_0)$, substituting the result under the integral, we obtain a volumetric IDE for the potential vector $\mathbf{A}$ with kernel G, which has the singularity $|\mathbf{r} - \mathbf{r}'|^{-1}$. The integral includes both $\mathbf{A}$ and the second derivatives of the components of the potential. The solution of this IDE requires the use of twice continuously differentiable basis functions, since the second derivatives are included under the integral, and the tangent components of the field must be continuous at the boundary of the body. An example of the transformation of a volume singular integral is given in the classical monograph [41] (see also [8]). The infinitesimal spherical neighborhood of the singular point is excluded, the integral over it is replaced by the surface integral over an infinitesimal sphere using the Ostrogradsky's formula, and the three-dimensional integral is understood in the sense of Cauchy's principal value as the limit for a remote spherical neighborhood as its radius tends to zero. As a result, an outside the integral term arises. To calculate the remaining integral, one can apply quadrature formulas or piecewise-constant FEs given during discretization on cubes, as well as smoother volumetric FEs. In this case, the diagonal matrix elements in the resulting system of linear algebraic elements are set to zero.

Next, we will transform singular IEs to weakly singular ones, i.e., e. to having kernels with reduced singularities, integrable in the usual sense, which allows the use of piecewise constant and other approximations The integral operators of such problems are Fredholm?s ones, and the problems are solvable [6–8]. Fundamentally, projection methods are substantiated for the equations of electrodynamics [35–37]. However, projection methods are not always convenient, and in some cases VIEs have advantages over them. For singular VIEs with the understanding of integrals in the sense described above, the Fredholm property and solvability [8,21–27] are also proved To simplify further calculations, we will consider transformations for a nonmagnetic body using the example of an VIE with respect to an electric field (1):

$$\mathbf{E}(\mathbf{r}) = \mathbf{E}^0(\mathbf{r}) + ik_0 \int\limits_V \hat{D}G(k, \mathbf{r}-\mathbf{r}')\hat{\chi}'^{\varepsilon}(\mathbf{r}')\mathbf{E}(\mathbf{r}')d^3r'. \quad (7)$$

Equation (2) then takes the form of

$$\mathbf{H}(\mathbf{r}) = \mathbf{H}^0(\mathbf{r}) + ik_0\eta_0^{-1} \int\limits_V \nabla\times G(k, \mathbf{r}-\mathbf{r}')\hat{\chi}'^{\varepsilon}(\mathbf{r}')\mathbf{E}(\mathbf{r}')d^3r'. \quad (8)$$

It makes it possible to calculate the magnetic field using the solution of VIE (7). Using Maxwell's n equation in the form $\mathbf{E}(\mathbf{r}) = -i\eta_0\hat{\varepsilon}^{-1}(\nabla\times\mathbf{H}(\mathbf{r}) - \mathbf{J}^0(\mathbf{r}))/k_0$ and substituting into the right side (8), we obtain the equation for the magnetic field. Here $\eta_0 = \sqrt{\mu_0/\varepsilon_0}$. For an isotropic body in vacuum, it has the form

$$\mathbf{H}(\mathbf{r}) = \mathbf{H}^0(\mathbf{r}) + \tilde{\mathbf{H}}^0(\mathbf{r}) + \int\limits_V \nabla\times\Big[G_0(k_0, \mathbf{r}-\mathbf{r}')(1-\varepsilon^{-1}(\mathbf{r}'))\nabla'\times\mathbf{H}(\mathbf{r}')\Big]d^3r'. \quad (9)$$

$$\tilde{\mathbf{H}}^0(\mathbf{r}) + \int\limits_V \nabla\times\Big[G(k, \mathbf{r}-\mathbf{r}')(\varepsilon'(\mathbf{r}')-1)\mathbf{J}^0(\mathbf{r}')\Big]d^3r'. \quad (10)$$

This is the IDE for the magnetic field. It is convenient for complex boundaries, since the magnetic field does not tolerate jumps on them, so continuous basis functions can be used. Dash bei operator $\nabla'\times$ means that it acts on dashed coordinates. For any vector function $\mathbf{F}$ we have

$$\nabla\times G_0(k_0, \mathbf{r}-\mathbf{r}')\mathbf{F}(\mathbf{r}') = -\nabla'\times\Big[G_0(k_0, \mathbf{r}-\mathbf{r}')\mathbf{F}(\mathbf{r}')\Big] + G_0(k_0, \mathbf{r}-\mathbf{r}')\nabla'\times\mathbf{F}(\mathbf{r}').$$

Applying the curl theorem ([42], pp. 175), we rewrite IDE (9) as

$$\mathbf{H}(\mathbf{r}) = \mathbf{H}^0(\mathbf{r}) + \tilde{\mathbf{H}}^0(\mathbf{r}) - \oint\limits_S G_0(k_0, \mathbf{r}-\mathbf{r}') \times\Big[(1-\varepsilon^{-1}(\mathbf{r}'))\nabla'\times\mathbf{H}(\mathbf{r}')\Big]\times\mathbf{v}(\mathbf{r}')d^2r' + \int\limits_V G_0(k_0, \mathbf{r}-\mathbf{r}')\nabla'\times\Big[(1-\varepsilon^{-1}(\mathbf{r}'))\nabla'\times\mathbf{H}(\mathbf{r}')\Big]d^3r'. \quad (11)$$

If IDE (9) requires continuously differentiable basis functions to solve, then IDE (11) requires twice continuously differentiable functions. Obviously, transformations can also be performed with a tensor DP.

For electromagnetic (photonic) crystals, the equations are modified simply by replacing the GF. The scalar GF of periodic sources, whose phases are shifted according to the Floquet-Bloch conditions by $\exp(-i(\mathbf{k}+\mathbf{g})(\mathbf{r}'))$, has the form

$$\tilde{G}(\mathbf{r}-\mathbf{r}') = \frac{1}{\Omega_0}\sum_{\mathbf{n}}\frac{\exp(-i(\mathbf{k}+\mathbf{g}_\mathbf{n})(\mathbf{r}-\mathbf{r}'))}{(\mathbf{k}+\mathbf{g}_\mathbf{n})^2 - k_0^2\tilde{\varepsilon}}. \quad (12)$$

Here $\Omega_0 = \mathbf{a}_1\cdot(\mathbf{a}_2\times\mathbf{a}_3)$ is volume of a unit cell of periodicity, $\mathbf{a}_1, \mathbf{a}_2, \mathbf{a}_3$ are translation vectors , $\mathbf{b}_1, \mathbf{b}_2, \mathbf{b}_3$ is-triplet of reciprocal lattice vectors: $\mathbf{a}_{kl}\mathbf{b}_l = 2\pi\delta_{kl}$, $\mathbf{b}_k = 2\pi(-1)^{P(klm)}\mathbf{a}_l\times\mathbf{a}_m/\Omega_0$, $P(klm) = \mp 1$ depending on the even/odd permutations, $bfg_n = n_1\mathbf{b}_1 + n_2\mathbf{b}_2 + n_3\mathbf{b}_3$, $\mathbf{n} = (n_1, n_2, n_3)$. For a box-shaped cell $\mathbf{a}_1 = (a_1, 0, 0)$, $\mathbf{a}_2 = (0, a_2, 0)$, $\mathbf{a}_3 = (0, 0, a_3)$, $\Omega_0 = a_1a_2a_3$, $\mathbf{g}_\mathbf{n} = (2\pi n_1/a1, 2\pi n_2/a_2, 2\pi n_3/a_3)$ and the sum is over all three indices $-\infty < n_k < \infty$. FG (12) satisfies the inhomogeneous Helmholtz equation with delta singularity $(\nabla^2 + k_0^2\tilde{\varepsilon})\tilde{G}(\mathbf{r}-\mathbf{r}')\exp(-i\mathbf{k}\mathbf{r}')$. The GF designated earlier has a spectral representation of type (12) in the form

$$G(\mathbf{r}-\mathbf{r}') = \frac{1}{(2\pi)^3}\int\frac{\exp(-i\mathbf{k}(\mathbf{r}-\mathbf{r}'))}{\mathbf{k}^2 - k_0^2\tilde{\varepsilon}}\,d^3k. \quad (13)$$

The triple integral over infinity is denoted by a single symbol. This representation is convenient for integration over coordinates, but requires the calculation of spectral integrals. The use of FG (12) requires the summation of the series. In a number of works, results were obtained on the rapid summation of similar series. Sometimes the following form of the GF, obtained by integration, for example, over the variable k_z by the residue method, can be useful:

$$G(\mathbf{r}-\mathbf{r}') = \frac{1}{8\pi^2}\int\limits_{-\infty}^{\infty}\frac{\exp(-ik_x(x-x')-ik_y(y-y') - i\tilde{k}_z(k_x,k_y)|z-z'|)}{i\tilde{k}_z(k_x, k_y)}\,dk_xdk_y. \quad (14)$$

Already here $\tilde{k}_z = \sqrt{k_0^2\tilde{\varepsilon} - k_x^2 - k_y^2}$. For damped (the English term is evanescent) waves in the direction of z $\tilde{k}_z = -i\sqrt{k_x^2 + k_y^2 - k_0^2\tilde{\varepsilon}}$. GFs are also often used

in shielded areas. It is quite easy to obtain a GFs for ideal screens [28], waveguides and resonators with ideal walls, in particular, a rectangular waveguide and a resonator [28,31,43], where it is constructed by the method of multiple images or using known eigenfunctions. If one formally denote the set of such functions $\varphi_n(\mathbf{r})$ and eigenvalues ω_n, then the GF is constructed as a resolution in the form of an expansion in $\varphi_n(\mathbf{r})\varphi_n^*(\mathbf{r}')/(\omega-\omega_n)$ [44]. Problems with dielectric half-spaces are much more complicated [28]. An example is the problem of a vertical Sommerfeld dipole. This also applies to the problem of a horizontal dipole. The presence of boundaries requires obtaining three solutions for three orientations of the electric dipole and three solutions for three orientations of the magnetic dipole. The GFs of layered structures are given in a large number of works, for example, in [45–50]. If the body has no magnetic properties ($\mu=1$), then the potential vector has components

$$A_\alpha^p(\mathbf{r})=\int\limits_{V_0} G_{\alpha\alpha}(k,\mathbf{r}-\mathbf{r}')J_\alpha^p(\mathbf{r}')d^3r',$$

$\alpha=x,y,z$, i.e. is determined not by a scalar, but by a diagonal tensor GF. With magnetic properties, one must also introduce a magnetic vector potential.

Since the transformation of equations to less singular kernels does not affect the free terms, we will carry them out using the example of VIE (1) for an open DR. Free oscillations of the DR correspond to the complex wave number $k_0=k_0'$. Instead of VIE (1), we will use the equivalent IDE [2]

$$\mathbf{E}(\mathbf{r})=\int\limits_V\Big\{k_0^2G_0(\mathbf{r}-\mathbf{r}')[\hat{\varepsilon}(\mathbf{r}')-\hat{I}]\mathbf{E}(\mathbf{r}')+\nabla G_0(\mathbf{r}-\mathbf{r}')\nabla'[(\hat{\varepsilon}(\mathbf{r}')-\hat{I})\mathbf{E}(\mathbf{r}')]\Big\}d^3r'+\oint\limits_S[\hat{\varepsilon}(\mathbf{r}')-\hat{I}](\mathbf{v}(\mathbf{r}')\mathbf{E}(\mathbf{r}'))\nabla'G_0(\mathbf{r}-\mathbf{r}')d^2r'. \quad (15)$$

Here $\mathbf{v}(\mathbf{r})\cdot\mathbf{E}(\mathbf{r})=E_v(\mathbf{r})$ is the normal component taken on the inner side of the surface, as is the quantity $\hat{\varepsilon}(\mathbf{r})$. IDE (15) is singular with an integrable singularity It is written for a vacuum GA, but can easily be rewritten for a GA of a dielectric base $G(k,\mathbf{r}-\mathbf{r}')$. This form is convenient for analyzing PCs or photonic-crystal waveguides with hole inclusions. In this case, the VIE should be solved only in the regions of holes (cavities), where the negative susceptibility $\chi'(\mathbf{r})=1/\tilde{\varepsilon}-1<0$ characterizes a hole in the dielectric space. The VIE (15) can be obtained using, for example, the Stretton-Chu formulas [3], or by directly applying vector integral theorems and transferring to (1) operations of differentiation from the kernel to the integration function [9,51]. In this case, one should use the relation $\nabla G_0(\mathbf{r}-\mathbf{r}')=-\nabla'G_0(\mathbf{r}-\mathbf{r}')$ and (Gauss) divergence theorem [9 ,40,51]. Since the point rushes to the surface from the inside, and the normal component of the electric field and the DP have a step on the surface S, in the surface integral in formula (15) one should take the limiting internal values on the surface. The external value corresponding to the vacuum will be denoted by the symbol „+“, and the internal value, respectively, as $\mathbf{E}^-$. The presence of a DP jump leads to the appearance on the surface density of the bound charge $\sigma(\mathbf{r})=\mathbf{v}\cdot\lfloor\hat{\varepsilon}(\mathbf{r})-\hat{I}\rfloor\mathbf{E}^-(\mathbf{r})$, $\mathbf{r}\in S$ due to the boundary condition $\mathbf{v}\cdot(\hat{\varepsilon}\mathbf{E}^--\mathbf{E}^+)=0$. In the case of scalar permeability, the IDE (15) can be converted into a volume-surface IE [9,51]

$$\mathbf{E}(\mathbf{r})=\int\limits_V\Big\{k_0^2G_0(\mathbf{r}-\mathbf{r}')[\varepsilon(\mathbf{r}')-1]\mathbf{E}(\mathbf{r}')-\varepsilon^{-1}(\mathbf{r}')[\mathbf{E}(\mathbf{r}')\nabla'\varepsilon(\mathbf{r}')]\nabla'G_0(\mathbf{r}-\mathbf{r}')\Big\}d^3r'+\oint\limits_S[\varepsilon(\mathbf{r}')-1](\mathbf{v}(\mathbf{r}')\mathbf{E}(\mathbf{r}'))\nabla'G_0(\mathbf{r}-\mathbf{r}')d^2r', \quad (16)$$

since then, due to the solenoidality of the vector $\varepsilon(\mathbf{r})\mathbf{E}(\mathbf{r})$, we have $\mathbf{E}(\mathbf{r})\nabla\varepsilon(\mathbf{r})+\varepsilon(\mathbf{r})\nabla\cdot\mathbf{E}(\mathbf{r})=0$ and $\nabla\cdot[\varepsilon(\mathbf{r})\mathbf{E}(\mathbf{r})-\mathbf{E}(\mathbf{r})]=\nabla\cdot\mathbf{E}(\mathbf{r})=\varepsilon^{-1}(\mathbf{r})\mathbf{E}(\mathbf{r})\nabla\varepsilon(\mathbf{r})$. In this case, a charge density arises on the surface $\sigma(\mathbf{r})=[\varepsilon(\mathbf{r})-1]E_v^-(\mathbf{r})=E_v^+(\mathbf{r})-E_v^-(\mathbf{r})$, i.e. the surface charge density is a scalar quantity and is expressed in terms of the step in field. If the DP is constant inside the volume, then the term with $\nabla'\varepsilon(\mathbf{r}')$ characterizing the bulk density vanishes, and the IE simplifies

$$\mathbf{E}(\mathbf{r})=k_0^2(\varepsilon-1)\int\limits_V G_0(\mathbf{r}-\mathbf{r}')\mathbf{E}(\mathbf{r}')d^3r'+(\varepsilon-1)\oint\limits_S E_v(\mathbf{r}')\nabla'G_0(\mathbf{r}-\mathbf{r}')d^3r'. \quad (17)$$

In the IE (17) $\nabla'G_0(\mathbf{r}-\mathbf{r}')=-\nabla G_0(\mathbf{r}-\mathbf{r}')$, so it has the form of representing the electric field in terms of the potential term with surface sources and potential and solenoidal terms with volumetric sources. Indeed, according to the Helmholtz theorem [42,52] $\mathbf{E}(\mathbf{r})=\nabla\times\mathbf{F}(\mathbf{r})-\nabla\Phi(\mathbf{r})$. This is a representation of the field through its potential and solenoidal parts. The problem is to formulate coupled equations for the potentials $\mathbf{F}(\mathbf{r})$ and $\Phi(\mathbf{r})$. Let?s consider the integral

$$\int\limits_V G_0(\mathbf{r}-\mathbf{r}')\nabla'\Phi(\mathbf{r}')d^3r'=\int\limits_V\Big\{\nabla'[G_0(\mathbf{r}-\mathbf{r}')\Phi(\mathbf{r}')]-\Phi(\mathbf{r}')\nabla G_0(\mathbf{r}-\mathbf{r}')\Big\}d^3r'.$$

It has the following form

$$-\nabla\int\limits_V G_0(\mathbf{r}-\mathbf{r}')\Phi(\mathbf{r}')d^3r'+\oint\limits_S\mathbf{v}(\mathbf{r}')[G_0(\mathbf{r}-\mathbf{r}')\Phi(\mathbf{r}')]d^2r'.$$

Here we have used the gradient theorem [42]. The gradient is explicitly distinguished in the first term, because it's potential one. The surface integral is a certain vector function with surface density $\mathbf{v}(\mathbf{r}')\Phi(\mathbf{r})$. Let's represent it as $\nabla \times \mathbf{L}(\mathbf{r}) - \nabla\Psi(\mathbf{r})$, $\mathbf{F} = k_0^2(\varepsilon - 1)\mathbf{L}$. Taking the divergence, we obtain the Poisson equation

$$\nabla^2\Psi(\mathbf{r}) = -\oint_S \mathbf{v}(\mathbf{r}')[\nabla G_0(\mathbf{r} - \mathbf{r}')\Phi(\mathbf{r}')]d^2r'. \qquad (18)$$

Taking the curl we also obtain the Poisson equation

$$\nabla^2\mathbf{F}(\mathbf{r}) = -k_0^2(\varepsilon - 1)\oint_S \mathbf{v}(\mathbf{r}') \times \nabla G_0(\mathbf{r} - \mathbf{r}')\Phi(\mathbf{r}')d^2r'. \qquad (19)$$

We have imposed the solenoidality condition on the vector $\mathbf{F}$. To find $\mathbf{F}$ and Ψ it is necessary to solve the Poisson equations, which can be formally written explicitly using the static GF $G_0(0, \mathbf{r} - \mathbf{r}') = (4\pi|\mathbf{r} - \mathbf{r}'|)^{-1}$ Then the integral is represented in the form

$$\oint_S \mathbf{v}(\mathbf{r}')[G_0(\mathbf{r} - \mathbf{r}')\Phi(\mathbf{r}')]d^2r' = \nabla \times \mathbf{L}(\mathbf{r}) - \nabla\Psi(\mathbf{r}),$$

and the equation for the potential Φ takes the form

$$\Phi(\mathbf{r}) = k_0^2(\varepsilon - 1)\Psi(\mathbf{r}) - k_0^2(\varepsilon - 1)\int_V G_0(\mathbf{r} - \mathbf{r}')\Phi(\mathbf{r}')d^3r' + (\varepsilon - 1)\oint_S E_v(\mathbf{r}')G_0(\mathbf{r} - \mathbf{r}')d^2r'. \qquad (20)$$

This potential is defined with an accuracy to a constant. The second volume integral in (17) has the representation

$$\int_V G_0(\mathbf{r} - \mathbf{r}')\nabla' \times \mathbf{F}(\mathbf{r}')d^3r' =$$

$$= \int_V \{\nabla' \times [G_0(\mathbf{r} - \mathbf{r}')\mathbf{F}(\mathbf{r}')] - \nabla G_0(\mathbf{r} - \mathbf{r}') \times \mathbf{F}(\mathbf{r}')\}d^2r'.$$

or

$$-\nabla \times \int_V G_0(\mathbf{r} - \mathbf{r}')\mathbf{F}(\mathbf{r}')d^3r' + \oint_S \mathbf{v}(\mathbf{r}') \times [G_0(\mathbf{r} - \mathbf{r}')\mathbf{F}(\mathbf{r}')]d^2r'.$$

Here the curl theorem is used. The theorems on gradient,curl and divergence (Gaussian) express the volume integrals of the action of these operators on certain functions in terms of surface integrals of these functions and allow one to transform the VIE. Such transformations (as well as Green's formulas) are a three-dimensional analogue of integration by parts. Breaking (17) into potential and solenoidal parts, we obtain

$$\mathbf{E}_0(\mathbf{r}) = k_0^2(\varepsilon - 1)\left[2\oint_S \mathbf{v}(\mathbf{r}') \times [G_0(\mathbf{r} - \mathbf{r}')\mathbf{F}(\mathbf{r}')]d^2r' - \int_V G_0(\mathbf{r} - \mathbf{r}')\nabla' \times \mathbf{F}(\mathbf{r}')d^3r'\right]. \qquad (21)$$

An exciting field, for example, of a plane wave, which is always solenoidal, is substituted into this equation. Taking into account the equation for the potential Φ, equation (21) can be interpreted as a volume-surface IDE for the function $\mathbf{F}(\mathbf{r})$. Relations (20) and (19) are linked paired equations. They define the electric field in terms of the introduced potentials $\mathbf{F}(\mathbf{r})$ and $\nabla\Phi(\mathbf{r})$. These equations must be solved simultaneously. The equations are linked via the surface integral in (20), since E_v depends on both potentials. Equations (20) and (21) for potentials have weakly singular kernels $G_0(\mathbf{r} - \mathbf{r}')$.

Surface integrals in (15) appear if the body has a sharp boundary, i.e., the function $\hat{\varepsilon}(\mathbf{r})$ on S is discontinuous and abruptly decreases to unity. If $\hat{\varepsilon}(\mathbf{r})$ is smooth and gradually decreases to unity in some inner surface layer, then $E_v^+(\mathbf{r}) = E_v^-(\mathbf{r})$ and the surface integral does not arise, but there is a volume charge density in the indicated layer. It is easy to show that, in the limit, as the thickness of such a layer decreases to zero, the volume integral over it is equivalent to the surface integral of the resulting jump of the normal field component. In diffraction problems, the equations should be supplemented with extraneous fields. Another approach to the transformation of equations is based on the singular IE [8,52–54] obtained from (1), (2) by selecting a singularity in the GF $G(k, \mathbf{r}) = G(0, \mathbf{r}) + \Delta G(k, (\mathbf{r}))$ and selection of the non-integral terms corresponding to it. They are distinguished by integrating over an infinitesimal ball surrounding the observation point using Ostrogradsky's theorem [54]. Such an IE does not contain surface integrals [8]. We will again carry out the transformation using the example of VIE (7) with a vacuum GF. Note that $G_0(k_0, \mathbf{r} - \mathbf{r}') = G_0(0, \mathbf{r} - \mathbf{r}') + \Delta G_0(k_0, \mathbf{r} - \mathbf{r}')$, where $\Delta G_0(k_0, \mathbf{r} - \mathbf{r}') = (4\pi R)^{-1}(\exp(-ik_0R) - 1)$, $R = |\mathbf{r} - \mathbf{r}'|$, or $\Delta G_0 = (4\pi R)^{-1}\lfloor -ik_0R - (k_0R)^2/2 + \ldots\rfloor$. The use of an approximate kernel is possible at low frequencies, when the discarded terms are small. The method of reduction to a singular VIE is based on integrating the second derivatives of the $\partial_{\alpha\alpha}^2 G_0(0, \mathbf{r} - \mathbf{r}')$ type over the solid sphere in the vicinity of the source point. As a result of applying the Ostrogradsky?s theorem, the term $-\hat{\chi}'^{\varepsilon}(\mathbf{r}')\mathbf{E}(\mathbf{r}')/3$ is extracted, and the equation becomes the form

$$\mathbf{E}(\mathbf{r})\left(\hat{I} + \hat{\chi}'^{\varepsilon}(\mathbf{r})\mathbf{E}(\mathbf{r})/3\right) = p.v.\int_V (\nabla \otimes \nabla + k_0^2\hat{I}) \times G_0(k_0, \mathbf{r} - \mathbf{r}')\hat{\chi}'^{\varepsilon}(\mathbf{r}')\mathbf{E}(\mathbf{r}')d^3r'. \qquad (22)$$

The integral is understood as the limit under conditions when infinitesimal neighborhood is removed of source point. Note that it is expedient to carry out this operation only for the diagonal terms of the operator $\nabla \otimes \nabla$.

Note one more possibility of transforming the equations in order to reduce the singularity of their kernels. For equations with respect to both fields, one can construct quadratic functionals by scalar multiplication by the bivector $(\mathbf{E}, \mathbf{H})$, or bilinear functionals by scalar multiplication by the bivector $(\tilde{\mathbf{E}}, b\tilde{f}H)$. If the bivector $(\mathbf{E}, \mathbf{H})$ is to be found, then the vector functions $\tilde{\mathbf{E}}$ and $\tilde{\mathbf{H}}$ and can be taken arbitrary. The degree of smoothness and boundary conditions for these weight functions $\nabla \otimes \nabla$ can be specified. In the case of twice differentiable such functions in the scalar product, the derivatives of the operator can be transferred both to the required fields under the integral and to weight-fields. In this case, it is possible to transfer the differential operator partially once or completely twice to weight-functions with tildes. In the latter case, the kernel G_0 appears. The same applies to equations for only electric or only magnetic fields. In this case, surface integrals arise. If the weight-functions still satisfy zero boundary conditions on the surfaces, this nullifies the surface integrals, simplifying the equations. Such trigonometric functions can be introduced, for example, to stimulate rectangular DRs.

3. Simulation of dielectric resonators

The complex resonant frequencies of an arbitrary DR in free space can be calculated based on any of the equations (15), (16), (22). Consider, for example, equation (15) for an isotropic and inhomogeneous DR:

$$\mathbf{E}(\mathbf{r}) = \int\limits_V \mathbf{E}(\mathbf{r}')\Big\{k_0^2 G_0(\mathbf{r}-\mathbf{r}')(\varepsilon(\mathbf{r}')-1) + \varepsilon^{-1}(\mathbf{r}')\nabla'\varepsilon(\mathbf{r}')\Big\}d^3r' + \oint\limits_S E_v(\mathbf{r}')(\varepsilon(\mathbf{r}')-1)\nabla' G_0(\mathbf{r}-\mathbf{r}')d^2r'. \quad (23)$$

Multiplying scalarly by $\mathbf{E}^*(\mathbf{r})$ and integrating, we get

$$k_0^2 = \frac{\int\limits_V |\mathbf{E}(\mathbf{r})|^2 d^3r - \int\limits_V\int\limits_V \mathbf{E}^*(\mathbf{r})\mathbf{E}(\mathbf{r}')\varepsilon^{-1}(\mathbf{r}')\nabla'\varepsilon(\mathbf{r}')d^3r'd^3r + \int\limits_V\oint\limits_S E_0(\mathbf{r}')(\varepsilon(\mathbf{r}')-1)\mathbf{E}^*(\mathbf{r})\nabla' G_0(\mathbf{r}-\mathbf{r}')d^2r'd^2r}{\int\limits_V\int\limits_V \mathbf{E}^*(\mathbf{r})\mathbf{E}(\mathbf{r}')G_0(\mathbf{r}-\mathbf{r}')(\varepsilon(\mathbf{r}')-1)d^3r'd^3r}.$$

This is a quadratic functional whose stationary value gives the square of the complex wave number, and its finding determines the field. It can be found iteratively together with the solution of VIE (23). A number of such functionals, as well as iterative algorithms for them, are given in the monograph [9]. The reduced functional and the VIE contain surface integrals, which is inconvenient. Let us consider the initial hypersingular VIE for such a DR:

$$\mathbf{E}(\mathbf{r}) = (\nabla \otimes \nabla + k_0^2)\int\limits_V G_0(\mathbf{r}-\mathbf{r}')(\varepsilon(\mathbf{r}')-1)\mathbf{E}(\mathbf{r}')d^3r'. \quad (24)$$

Let's choose a function $\tilde{\mathbf{E}}(\mathbf{r})$ such that its normal component vanishes on the DR surface. Then scalar multiplication gives the functional

$$k_0^2 = \frac{\int\limits_V \tilde{\mathbf{E}}^*(\mathbf{r})\mathbf{E}(\mathbf{r})d^3r + \int\limits_V\int\limits_V \tilde{\mathbf{E}}^*(\mathbf{r})\nabla G_0(\mathbf{r}-\mathbf{r}')(\varepsilon(\mathbf{r}')-1)\mathbf{E}(\mathbf{r}')d^3r'}{\int\limits_V\int\limits_V \tilde{\mathbf{E}}^*(\mathbf{r})\mathbf{E}(\mathbf{r}')G_0(\mathbf{r}-\mathbf{r}')(\varepsilon(\mathbf{r}')-1)d^3r'}. \quad (25)$$

Its extremum can be found using basis functions and weight functions $\mathbf{E}_n(\mathbf{r})$. In this case, the system of linear equations should be solved together with iterations in (25). Before each iteration, the electric field should be normalized [9].

Let's consider cylindrical DRs, for which we use the representation of the GF in a cylindrical coordinate system [28]. One way to do this is to replace the variables $x = \rho\cos(\varphi)$, $y = \rho\sin(\varphi)$ in the corresponding Cartesian representations, for example,

$$G(\rho, \varphi, z\,|\rho', \varphi', z') = (4\pi R)^{-1}\exp(-jkR),$$
$$R = \left(\rho^2 + \rho'^2 - 2\rho\rho'\cos(\varphi-\varphi') + (z-z')^2\right). \quad (26)$$

It is possible to perform the above replacement in other GF representations given by the relations given in [28], for example, formulas 2.8 and 2.14, or use the representation 2.15 (hereinafter, all similar references will correspond to the indicated work). However, it is often more convenient to use direct representations of the GF in a cylindrical system (formulas 2.17, 2.18, 2.20, 2.21 and 2.22). The presence of several types of GF representations creates convenience when calculating integrals in matrix elements, since it is possible to choose the most appropriate formula for which they are calculated most simply, and also allows you to solve the problem with several algorithms. Upon transition to a cylindrical coordinate system, the vector-potential $\mathbf{A}$ and the vector $\mathbf{E}$ are transformed according to formulas 2.63, while the VIE becomes

$$E_\rho(\rho, \varphi, z) = k^2\int\limits_V G(\mathbf{r}-\mathbf{r}')[\varepsilon(\mathbf{r}')-1] \times \left\{E_\rho(\mathbf{r}')\cos(\varphi-\varphi') + E_\varphi(\mathbf{r}')\sin(\varphi-\varphi')\right\}d^3r' - \int\limits_V\left\{\varepsilon^{-1}(\mathbf{r}')[\mathbf{E}(\mathbf{r}')\nabla'\varepsilon(\mathbf{r}')]\frac{\partial G(\mathbf{r}-\mathbf{r}')}{\partial\rho'}\right\}d^3r' + \oint[\varepsilon(\mathbf{r}')-1](\mathbf{v}(\mathbf{r}')\mathbf{E}(\mathbf{r}'))\frac{\partial G(\mathbf{r}-\mathbf{r}')}{\partial\rho'}\,d^2r', \quad (27)$$

$$E_\rho(\rho,\varphi,z)=k^2\int\limits_V G(\mathbf{r}-\mathbf{r}')[\varepsilon(\mathbf{r}')-1]$$
$$\times\left\{E_\varphi(\mathbf{r}')\cos(\varphi-\varphi')-E_\rho(\mathbf{r}')\sin(\varphi-\varphi')\right\}d^3r'$$
$$-\int\limits_V\left\{\varepsilon^{-1}(\mathbf{r}')[\mathbf{E}(\mathbf{r}')\nabla'\varepsilon(\mathbf{r}')]\,\frac{\partial G(\mathbf{r}-\mathbf{r}')}{\rho\partial\varphi'}\right\}d^3r'$$
$$+\oint[\varepsilon(\mathbf{r}-\mathbf{r}')-1](\mathbf{v}(\mathbf{r}-\mathbf{r}')\mathbf{E}(\mathbf{r}-\mathbf{r}'))\frac{\partial G(\mathbf{r}-\mathbf{r}')}{\rho\partial\varphi'}\,d^2r', \tag{28}$$

$$E_z(\rho,\varphi,z)=k^2\int\limits_V G(\mathbf{r}-\mathbf{r}')[\varepsilon(\mathbf{r}')-1]E_z(\mathbf{r}')d^3r'$$
$$-\int\limits_V\left\{\varepsilon^{-1}(\mathbf{r}')[\mathbf{E}(\mathbf{r}')\nabla'\varepsilon(\mathbf{r}')]\,\frac{\partial G(\mathbf{r}')}{\partial z'}\right\}d^3r'$$
$$+\oint[\varepsilon(\mathbf{r}')-1](\mathbf{v}(\mathbf{r}')\mathbf{E}(\mathbf{r}'))\frac{\partial G(\mathbf{r}')}{\partial z'}\,d^2r'. \tag{29}$$

In the coupled IE (27)–(29), for compactness of notation, the coordinates $\mathbf{r}$ and $\mathbf{r}'$ are used, which should be considered in a cylindrical system. The volume element has the form $d^3r'=\rho'd\rho'd\varphi'dz'$, and the form of the surface element d^2r' depends on the coordinate of the point on the cylinder.

In the case when the field does not depend on the coordinate φ, these GFs can be simplified by integrating over the angle. Let, for example, azimuthally symmetric H-oscillations of an isotropic cylindrical DR of radius r_0 and height h be considered. Then only the E_φ-component is nonzero, and IE (5)–(7) takes the form [4]

$$E_\varphi(\rho,z)=k^2\int\limits_{S_M}(\varepsilon(\rho',z')-1)\bar{G}(\rho,z|\rho',z')\rho'd\rho'dz', \tag{30}$$

where S_M –is the meridian section $0\le\rho\le r_0$, $|z|\le h/2$, and the kernel has the representation

$$\bar{G}(\rho,z|\rho'z')=\int\limits_0^{2\pi}\cos(\varphi-\varphi')G(\rho,\varphi,z|\rho',\varphi',z')d\varphi'. \tag{31}$$

GF (31) does not depend on φ and is also represented by a double integral of type (31) over $(0,\pi)$. Indeed, let?s make a change of variables $\vartheta=\varphi'-\varphi$ in (31). Since R and G are periodic in ϑ with period 2π, the value of the integral (31) over the domain $(-\varphi,2\pi-\varphi)$ does not depend on values φ. In [4] it is proposed to calculate GF (9) by expanding the exponent in (4) into a series and expressing recursively obtained integrals in terms of elliptic integrals of the first and second kind. But for GF (31) there are other representations, for example, it follows from formula 2.18

$$\bar{G}(\rho,z|\rho',z')=\frac{1}{2}\int\limits_0^\infty$$
$$\times\frac{J_1(\chi\rho)J_1(\chi\rho')\exp(-\sqrt{\chi^2-k^2}|z-z'|)}{\sqrt{\chi^2-k^2}}\,\chi d\chi, \tag{32}$$

and from 2.22, respectively, we obtain

$$\bar{G}(\rho,z|\rho',z')=$$
$$=\frac{-j}{4}\int\limits_0^\infty\begin{Bmatrix}H_1^{(2)}(\sqrt{k^2-\gamma^2}\rho')J_1(\sqrt{k^2-\gamma^2}\rho)\\ J_1(\sqrt{k^2-\gamma^2}\rho')H_1^{(2)}(\sqrt{k^2-\gamma^2}\rho)\end{Bmatrix}$$
$$\times\exp(-j\gamma(z-z'))d\gamma. \tag{33}$$

In (33) the upper value in curly bracket should be taken at $\rho<\rho'$, and the lower should be taken at $\rho>\rho'$ The GF (31)–(33) representations are convenient for the analysis of azimuthally symmetric $H_{0n\delta}$ and $E_{0n\delta}$ vibration types. For hybrid $HE_{mn\delta}$ and $EH_{mn\delta}$ types, the GFs have the form 2.18 and 2.22, in the sums of which it is necessary to leave only one azimuthal term $\exp(-jm(\varphi-\varphi'))$.

A large number of works have been devoted to methods of DR analysis (see, for example, monographs [55,56] and the list of references there), and various methods have been used: approximate heuristic methods (for example, the magnetic wall method), perturbation theory (decomposition by a small parameter), the method of partial domains (MPO), or matching, with obtaining surface integral equations, the method of VIE [4]. Of these, the last two methods are rigorous, the latter being the most universal, since it allows one to analyze inhomogeneous DRs of arbitrary shape. However, it has not been adequately considered in the literature. In the publication [4] it is formulated for the $H_{01\delta}$ mode of a homogeneous cylindrical DR, and the perturbation theory is ultimately used. Due to the complexity of determining the expansion coefficients, the MPO for a cylindrical DR has not been rigorously implemented, but has been replaced by an approximate approach [55], which does not allow one to determine the radiative quality factors of oscillations. Works [56–63] on DR simulation should be noted. The VIE method for the analysis of DR has been used in a number of works [4,5,9,59,63–66]. In [65] the results for a rectangular DR are given, where the sines and cosines of the arguments k_xx, k_yy and k_zz are used as basis functions, satisfying the Helmholtz equation inside the dielectric, i.e., for $k_x^2+k_y^2+k_z^2=k_0^2$ $varepsilon$. In addition, the condition of solenoidality of the electric field inside the rectangle was used, which made it possible to significantly reduce the number of basis functions used, that is, the algebraic dimensionality of the problem. In [66] the VEI method for a rectangular DR is also used, and the $H_{01\delta}$ and H_{011} modes of a homogeneous and inhomogeneous cylindrical DR are also simulated. Fig. 1, 2 show the

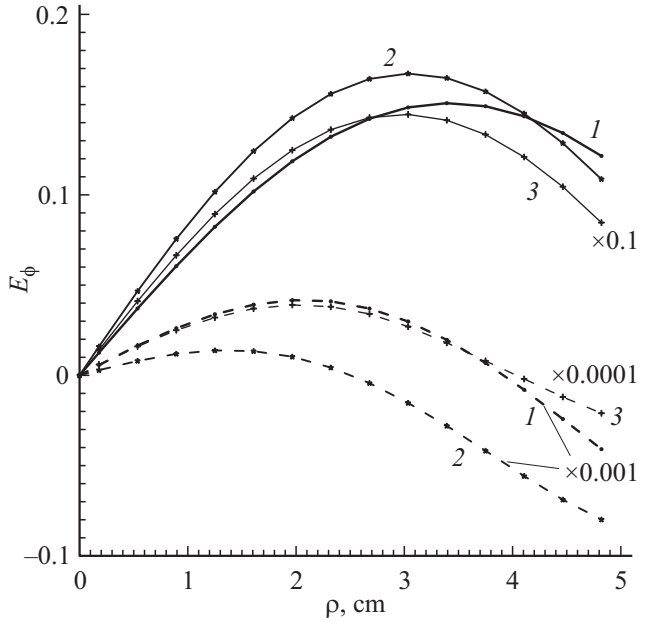

Figure 1. Dependences of $\mathrm{Re}(E_\varphi)$ (solid curves) and $\mathrm{Im}(E_\varphi)$ (dashed curves) on coordinate ρ for cylindrical DR $\varepsilon = 100$, $r_0 = h = 5$ mm: *1* is mode $H_{01\delta}$ at $z = 0.09$; *2* is mode H_{011} at $z = 2.41$; *3* is mode H_{011} at $z = 0.09$.

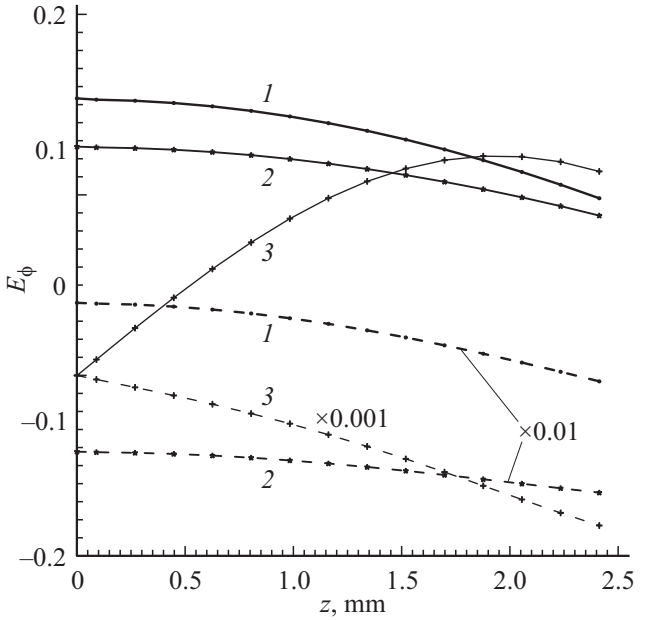

Figure 2. $\mathrm{Re}(E_\varphi)$ (solid curves) and $\mathrm{Im}(E_\varphi)$ (dashed curves) on coordinate z for a cylindrical DR $\varepsilon = 100$, $r_0 = h =$ mm: *1, 2* is mode $H_{01\delta}$ at $\rho = 3.4$ and $\rho = 1.66$ mm; *2* is mode H_{011} at $\rho = 4.46$ mm.

Table 1. Dependence of the resonant frequency of modes and on the shape of a homogeneous cylindrical DR with $\varepsilon = 50$, $h = 5$ mm

Mode	Radius to height ratio r_0/h					
	0.4	0.6	0.8	1.0	1.2	1.4
	Frequencies in GHz					
$H_{01\delta}$	9.01	6.22	5.23	4.41	3.96	3.57
H_{011}	11.65	9.15	7.97	7.53	7.10	6.72

field distributions at resonance for the $H_{01\delta}$ mode of a homogeneous cylindrical DR. The method of direct iteration in the form of the method of successive approximations (MSA) and the method of minimum residuals with freezing the values of the GF from the spectral parameter at the previous step were used, applied to the IE and the strict characteristic equation. One-dimensional piecewise-constant and differentiable (in the form of second-order polynomials) FEs, given by three nodes, were used. Both methods converge to the same results in several iterations with respect to the complex parameter k_0. Resonance frequencies and quality factors are given in Tables 1 and 2.

The study of the convergence of the algorithm is shown in Fig. 3. In the considered example, the MSA converges quickly, but for complex configurations, iterations may not converge for all initial values. The simple iteration method for finding the root of the equation $f(x) = 0$ can be written as $x_n = x_{n-1} - \tau_n f(x_{n-1})$, while for its iteration parameter $\tau_n = \tau$ is the same all the time. In the work [67] an

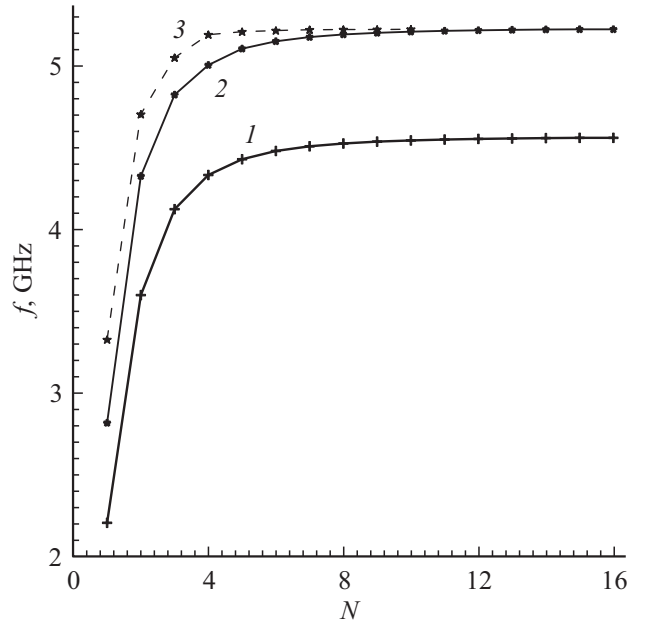

Figure 3. Convergence of the results for eigenfrequencies f of the cylindrical DR on the number of basis functions N for piecewise-constant (*1, 2*) and polynomial quadratic (*3*) approximations for $\varepsilon = 38$, $r_0 = 5$ mm: $h = 7$ mm (*1*); $h = 4$ mm (*2, 3*).

iteration method is developed with a correction at each step of the complex iteration parameter τ_n, which ensures unconditional convergence. An alternative to the algorithm can be projection methods for VIE, which lead to the need to search for complex roots of determinants of large orders.

Table 2. Dependence of the radiative quality factor of the $H_{01\delta}$ and H_{011} modes of a homogeneous cylindrical DP oat the dielectric permittivity for $r_0 = 5$ mm, $h = 7$ mm

Mode	Dielectric permeability ε					
	10.0	20.0	40.0	80.0	160.0	320.0
	Quality factor Q					
$H_{01\delta}$	4.2	12.4	66.1	125.3	251.0	505.7
H_{011}	45.1	382.1	1250.3	2802.5	5621.2	12250.7

The VIE approach for azimuthally symmetric modes of cylindrical DRs was also used in [59]. The problems of DR with ideal flat screens are solved on the basis of the VIE by constructing the GF by the image method. To analyze spherical DRs, one should use the expansion in terms of spherical harmonics ([28,68–71]). The distribution of fields in a cylindrical DR shows that it does not correspond to the distribution with magnetic walls in both coordinates ρ and z, i.e. e. in the H_{0mn} mode classification. Such a classification corresponds to a screened DR with the number of half-waves m in the radial coordinate and n in the coordinate z. Open resonator with radius a and height b, from the Helmholtz equation implies $k_{\rho m}^2 + k_{zn}^2 = \omega_{mn}^2 \varepsilon / c^2$, so the indices in the relations $k_{\rho m} = m\pi/a$, $k_{zn} = n\pi/b$ cannot be integer: the conditions of the magnetic wall are not satisfied, and the field goes beyond the boundaries of the DR. Moreover, since the indices are related to the complex resonant frequency, they must be complex. These parameters are included in the complex Bessel functions describing the modes. Usually in the literature a very conditional classification $H_{0m\delta}$ is used, in which $0 < \delta < 1$ is considered. This classification corresponds well to the case of a large DP, when the field almost does not go beyond the DR, and the frequencies are almost real. The complex frequencies $\omega_n = \omega_n' + j\omega_n''$ define time-damped free oscillations $\mathbf{E}_n$ with number n, while $\omega_n'' > 0$. Then for the eigen(resonance) mode in the far zone we have

$$\mathbf{E}_n(\mathbf{r}) = \frac{\omega_n^2 \exp(-j\omega_n r/c)}{4\pi r c^2} \mathbf{F}(\theta, \varphi). \qquad (34)$$

The vector directional pattern $\mathbf{F}$ depends on the distribution of the electric field in the volume V and determines the distribution of the DR radiation in the far zone for the indicated mode [72]:

$$\mathbf{F}(\theta, \varphi) =$$

$$= \int_V e^{j\omega_n r' \cos(\psi)/c} \lfloor \hat{\varepsilon}(\mathbf{r}') - \hat{I} \rfloor \mathbf{E}_n(\mathbf{r}') r'^2 \sin(\theta') dr' d\theta' d\varphi'.$$

Here

$$\cos(\psi) = \cos(\theta)\cos(\theta') + \sin(\theta)\sin(\theta')\cos(\varphi - \varphi'').$$

As can be seen, the eigenmode fields (34) increase at infinity [73], which is due to their exponential decrease in time. As shown in [73], the energy conservation law holds as follows: longer distances correspond to earlier emission times (determined by r/c being delayed). At these early moments, the energy of oscillations in volume V was exponentially greater [73] due to exponential damping. The modulus of the function (34) has a minimum at the point $r_n = c/\omega_n''$. If this point corresponds to the far zone, then the field can have an oscillatory character in a given direction inside V, then, as it moves away from the DR, its modulus decreases to the specified radius, and then begins to increase. For high-quality oscillations $r_n \gg a$, which justifies the approximate method of calculating the real natural frequencies [56] by replacing the fields (34) with decreasing ones. Spherical DRs are considered in the works [4,57,58]/ B Approximate solution is obtained as an expansion in a $1/\varepsilon$ small parameter. It works well with a large DP. Rigorous dispersion equation was obtained in [58]. For a given frequency, it has two solutions in the form of a converging and diverging wave. In [58] one of its two solutions is erroneously taken as the solution decreasing at infinity. In fact, it is a converging spherical wave. The problem of free oscillations of a spherical DR is related to the solution of the inhomogeneous Maxwell equations of the Mie problem of diffraction by a dielectric solid sphere. In the work [4] the VIE method is used for the numerical determination of the resonant frequencies and Q-factors of the $H_{01\delta}$ mode. DRs are often used as radiators in antennas. Stationary excitation of such emitters at a given frequency leads to decreasing fields in the far field zone. Non-stationary radiation over a finite time also leads to fields decreasing at infinity.

Let us also present the VIE with respect to the magnetic field. We proceed from equation (24). We take the curl of this equation, introduce this operator under the integral and use the curl theorem:

$$\nabla \times \mathbf{E}(\mathbf{r}) = k_0^2 \int_V G_0(\mathbf{r} - \mathbf{r}') \nabla' \times [(\varepsilon(\mathbf{r}') - 1)\mathbf{E}(\mathbf{r})] d^3 r'$$

$$- k_0^2 \oint_S G_0(\mathbf{r} - \mathbf{r}') \mathbf{v}(\mathbf{r}') \times [(\varepsilon(\mathbf{r}') - 1)\mathbf{E}(\mathbf{r}')] d^2 r'.$$

We have

$$\nabla \times [(\varepsilon(\mathbf{r}) - 1)\mathbf{E}(\mathbf{r})] = \nabla\varepsilon(\mathbf{r}) \times \mathbf{E}(\mathbf{r}) + (\varepsilon(\mathbf{r}) - 1)\nabla \times \mathbf{E}(\mathbf{r}).$$

Using Maxwell's equations, we substitute $\nabla \times \mathbf{E}(\mathbf{r}) = -i\omega\mu_0 \mathbf{H}(\mathbf{r})$ and $\mathbf{E}(\mathbf{r}) = -i\nabla \times \mathbf{H}(\mathbf{r})/(\omega\varepsilon_0\varepsilon)$. As a result, we obtain the IDE with respect to the magnetic field

$$\mathbf{H}(\mathbf{r}) = \int_V G_0(\mathbf{r} - \mathbf{r}')$$

$$\times \left[\nabla \times \mathbf{H}(\mathbf{r}) \varepsilon^{-1} \nabla' \varepsilon(\mathbf{r}') + k_0^2 (\varepsilon(\mathbf{r}') - 1)\mathbf{H}(\mathbf{r}') \right] d^3 r'$$

$$- \frac{k_0^2}{\omega\mu_0} \oint_S G_0(\mathbf{r} - \mathbf{r}') \mathbf{v}(\mathbf{r}') \times [(\varepsilon(\mathbf{r}') - 1)\nabla' \mathbf{H}(\mathbf{r}')] d^2 r'.$$

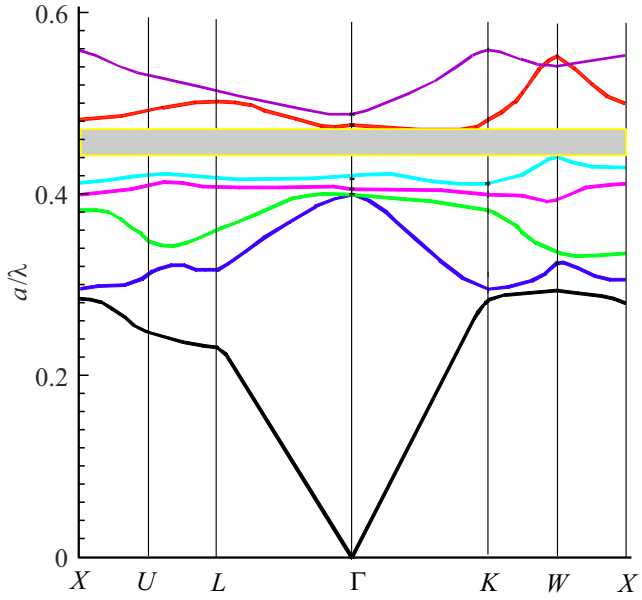

Figure 4. The band structure of a PC of the type inverted opal with DP base of $\tilde{\varepsilon} = 3.9$ and a filling factor of $f = 0.35$. Hollow spheres were discretized by inscribed cubic finite elements. The bandgap zone is shown in grey.

If, on the basis of this equation, a DK with uniform filling is analyzed, then the equation is simplified:

Fig. 4 shows an example of calculating the dispersive band structure of a PC of the inverted opal type in the form of loosely packed spherical cavities (metaatoms) in a base with $\tilde{\varepsilon} = 4$ DP. It should be noted that the VIE method has good convergence compared to other methods, for example, plane waves with respect to the number of basis functions. The calculation of GF (12) can be significantly accelerated by applying fast summation methods The periodic GF can be calculated differently based on the periodic translation to the vector $n_x a_x \mathbf{x}_0 + n_y a_y \mathbf{y}_0 + n_z a_z \mathbf{z}_0$ and the summation of the FG of the free space $G(k, \mathbf{r} - \mathbf{r}')$ with the corresponding phase factors $\exp(-i(k_x a_x n_x + k_y a_y n_y + k_z a_z n_z))$. By applying the Poisson summation formula, we can prove the equivalence of both approaches to calculating the GF.

4. Waves in dielectric and photonic-crystal waveguides

Waveguide structures (waveguides) regular along the z axis are invariant with respect to translations; therefore, they support modes with the dependence $\exp(i\omega t - i\gamma(\omega)z)$. Differentiation with respect to z in Maxwell's equations reduces to multiplication by $-i\gamma$, i.e. the boundary value problem becomes two-dimensional in cross section. Accordingly, the goal is to determine the dispersion of $\gamma(\omega)$ modes, of which there are infinitely many. The problem for a dielectric waveguide (DW) is reduced to a two-dimensional VIE with respect to the cross section S. For open DWs, the cross section S is usually bounded, and the scalar GF, up to a factor of $-i/4$, is proportional to the Hankel function of the second kind in the argument $\kappa|\mathbf{r}_\tau - \mathbf{r}'_\tau|$, i.e. e. has a logarithmic feature. The index τ corresponds to the transverse coordinates x, y. With a real transverse wavenumber κ and with the chosen time dependence $\exp(i\omega t)$, this Hankel function in the far field zone is a diverging cylindrical wave. The index τ corresponds to the transverse coordinates x, y. For shielded DWs, ideally conducting screens are usually considered. In this case, the GF is constructed by the image method. Thus, for a rectangular screen, a two-dimensional infinite system of images arises, given by a two-dimensional series, an example of which can be found in [31]. In the case of ideal magnetic walls, the image method can also be used, as in the case of a magnetic dipole with respect to both types of walls. Below, we will consider only open DWs. It is convenient to use a two-dimensional GF [28]

$$G_\tau(\omega, \gamma, \mathbf{r}_\tau) = \frac{1}{4\pi^2} \int\limits_{-\infty}^{\infty} \frac{\exp(-ik_x x - ik_y y)}{k_x^2 + k_y^2 - (k_0^2 - \gamma^2(\omega))} dk_x dk_y. \tag{35}$$

Here, the source is at the origin of coordinates. Bringing it to the form

$$G_\tau(\omega, \gamma, \mathbf{r}_\tau) = \frac{1}{4\pi} \int\limits_{-\infty}^{\infty} \times \frac{\exp\left(-ik_x x - \sqrt{\gamma^2(\omega) + k_x^2 - k_0^2}|y - y'|\right)}{\sqrt{\gamma^2(\omega) + k_x^2 - k_0^2}} dk_x dk_y, \tag{36}$$

we obtain the well-known representation GF [28] for the DW in terms of the Hankel function of the second kind.

$$G_\tau(\omega, \gamma, \mathbf{r} - \mathbf{r}'_\tau) = -\frac{i}{4} H_0^{(2)}(\kappa R_\tau). \tag{37}$$

In it $\kappa = \sqrt{k_0^2 - \gamma^2(\omega)}$ is spectral parameter or transverse wave number, $R_\tau = |\mathbf{r}_\tau - \mathbf{r}'_\tau| = \sqrt{(x - x')^2 + (y - y')^2}$. The form (37) is convenient for fast leaky waves $k_0 > \mathrm{Re}(\gamma(\omega))$. Even if dissipation in the dielectric is neglected, in this case we obtain complex $\gamma(\omega)$. For slow surface waves $k_0^2 < \gamma^2(\omega)$ and the GF is expressed in terms of the MacDonald function: $G_\tau(\omega, \gamma, \mathbf{r}_\tau - \mathbf{r}'_\tau) = (2\pi)^{-1} K_0(qR_\tau)$. It is convenient to take the spectral parameter in the form $q = \sqrt{\gamma^2(\omega) - k_0^2} > 0$. In a neighborhood of a singular point, we have

$$G_\tau(\omega, \gamma, \mathbf{r}_\tau - \mathbf{r}'_\tau) \approx -i\left(1 - 2i(C + \ln(\kappa R_\tau/2))/\pi\right)/4$$

$$\approx -\ln(R_\tau)/(2\pi).$$

Here we use the representation of the Macdonald function with a small argument. he second derivative of the logarithmic potential $\Phi = \ln(R\tau)$ is not an integrable function

in the usual sense. Let?s calculate the second derivative of the potential from some continuously differentiable charge density $\rho(\mathbf{r}_\tau)$ in a two-dimensional region S in the case when the observation point belongs to this region, i.e. value

$$\partial_x^2 \int\limits_S \ln\left(\sqrt{(x-x')^2+(y-y')^2}\right)\rho(x',y')dx'dy'.$$

Further, the derivation of formulas is similar to the derivation considered in paragraph 5 of Chapter 4 of the work [54]. Let's decompose the integral into two. We take the first one along a circle of radius δ, in the center of which there is a point of interest to us (we denote it by $\mathbf{r}_{0\tau}) = (x_0, y_0)$), and the second integral we take along the remaining region $\tilde{S}$:

$$I = I_1 + I_1 = \int\limits_{S_\delta} \ln(R_\tau)\rho(r'_\tau)dx'dy' + \int\limits_{\tilde{S}} \ln(R_\tau)\rho(r'_\tau)dx'dy'.$$

The second derivative of the second integral is calculated in the usual sense. Since $\partial_x R_\tau = -\partial_{x'} R_\tau$, we transform the first derivative of the first integral

$$\partial_x I_1 = -\int\limits_{S_\delta} \rho(r'_\tau)\partial_{x'} \ln(R_\tau)dx'dy' =$$

$$-\oint\limits_{L_\delta} \rho(r'_\tau)\ln(R_\tau)\cos(\varphi)dl + \int\limits_{S_\delta} \ln(R_\tau)\partial_{x'}\rho(r'_\tau)dx'dy'.$$

Here $gl = \delta d\varphi$, $\cos(\varphi) = (x-x')/R_\tau$. It is a differentiable function. Calculating the second derivative

$$\partial_x^2 I_1 = -\oint\limits_{L_\delta} \rho(r'_\tau)\partial_x \ln(R_\tau)\cos(\varphi)dl$$

$$+\int\limits_{S_\delta} \partial_x \ln(R_\tau)\partial_{x'}\rho(r'_\tau)dx'dy'$$

and estimating the integrals, in the limit of $\delta \to 0$ we obtain the result $\partial_x^2 I_1 = \pi\rho(r_{0\tau})$. Indeed, the second integral has an upper bound $2\pi\delta \max(\partial_{x'}\rho)$, while the first one is calculated from mean value theorem. Thus, in a two-dimensional singular VIE with respect to the electric field $\mathbf{E}(\mathbf{r}_\tau)$ under the action of the operator $\nabla_\tau \otimes \nabla_\tau$ with the definition of the integral in the sense of principal value indicated above, the non-integral term $-\mathbf{E}(\mathbf{r}_{0\tau})/2$ arises (recall that for a three-dimensional VIE it is equal to $-\mathbf{E}(\mathbf{r}_0)/3$). Then we can put $\mathbf{r}_{0\tau} = \mathbf{r}_\tau$, i.e. consider any point on S. For a lossy dielectric, both the Hankel function and the MacDonald function are complex. The modes of such a DW are classified as inflow ones and leaky ones [9,30]. The leaky mode is characterized by the value $\mathrm{Re}(\kappa) = \mathrm{Re}\sqrt{k_0^2 - \gamma^2(\omega)}$. Determining $\mathrm{Re}(\gamma)$, we get the leaky-mode-angle $\vartheta = \arctan(\mathrm{Re}(\kappa)/\mathrm{Re}(\gamma))$. If it is negative, the wave is leaky, i.e., energy fluence goes at an angle from vacuum to the dielectric. The boundary

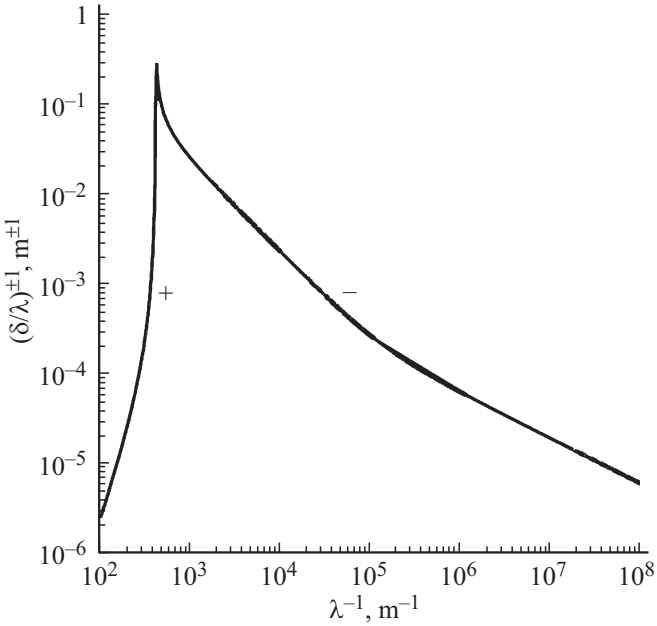

Figure 5. The depth of penetration into silver normalized to the wavelength $(+)$ and its reciprocal $(-)$ depending on the reciprocal wavelength λ^{-1}.

between fast and slow waves is determined by the condition $\gamma = k_0$, which plays the same role for DE as the critical frequencies in hollow waveguides. The wave under the condition $\gamma = k_0$ travels at the speed of light, it is not transversely limited, and all its energy is transferred in vacuum. The boundary between inflow- and leaky mode is determined by the condition $\vartheta = 0$. In particular, fast inflowing waves are surface waves of the Sommerfeld-Zenneck type in dissipative waveguide structures [9,30]. Slow inflowing waves are surface plasmons along strongly dissipative structures. Metals are described as dissipative dielectrics, and the depth of penetration of the field into the metal strongly depends on the type of skin effect and frequency. The calculation of the wavelength-normalized penetration depth for silver is given in Fig. 5 [29]. In the entire range, it does not fall below 200 nm, and has a wide minimum in the wavelength range from 5 μm to 1 mm. Therefore, thin metal films and nanostructures, the transverse dimensions of which are less than 200 nm, can be described by VIE. In this case, for very thin films, the field in the transverse direction remains almost unchanged. Such films can even be described by surface conductivity.

The transition from slow to fast plasmons takes place in the $-1 < \varepsilon' < 0$ region, which corresponds to the optical or IR range for metals. Thus, the VIE method is also applicable to dielectric structures with thin metal films or nanosized inclusions. In particular, it can be used to simulate localized plasmons in small metal particles or plasmonic electromagnetic crystals (PCs with small metal inclusions). It should be noted here that equation (22) for isotropic homogeneous metal particles in vacuum takes the

form

$$\mathbf{E}(\mathbf{r})(2+\varepsilon)/3 = (\varepsilon-1)p.v.\int\limits_V (\nabla\otimes\nabla + k_0^2\hat{I}) \times G_0(k_0, \mathbf{r}-\mathbf{r}')\mathbf{E}(\mathbf{r}')d^3r'.$$

It cannot be solved for $\varepsilon = -2$ because of the appearance of a pole. In reality, the DP of a metal is complex, but if the dissipation is small, the point $\varepsilon' = \mathrm{Re}(\varepsilon) = -2$ is the point of condensation of the oscillation spectrum of localized plasmons [74]. In this region, with low losses, other VIEs should be used.

Since now the polarization current has the form $\mathbf{J}^p(x,y) = i\omega\varepsilon_0[\varepsilon(x,y)-1]\mathbf{E}(x,y)$, then the two-dimensional VIE are formulated according to the type of the above equations in the region of the cross section S. Although we use fields in the equations that depend on transverse coordinates, in reality all fields also have the dependence $\exp(-i\gamma z)$. This means that you should use the operator $\nabla\otimes\nabla = (\nabla_\tau + \mathbf{z}_0\gamma)\otimes(\nabla_\tau + \mathbf{z}_0\gamma)$, where $\nabla_\tau = \mathbf{x}_0\partial_x + \mathbf{y}_0\partial_y$. By separating out the part $\nabla_\tau\otimes\nabla_\tau$ in this operator, one can transform the hypersingular VIE with the integral term distinguished outside the integral in the sense of the principal value. Other possible types of VIE are obtained by transformations by transferring the operator ∇_τ to integrands. Such VIEs become loaded with contour integrals containing derivatives. Therefore, they should be interpreted as IDE. Thus, the equations directly include the parameter γ, k_0, and the spectral parameter $\kappa = \sqrt{k_0^2 - \gamma^2(\omega)}$ or $q = \sqrt{\gamma^2(\omega) - k_0^2}$. In two-dimensional PCs in the form of a set of dielectric cylinders periodically located in the cross section, one can use the reduced GF (35) transformed using the periodicity:

$$\tilde{G}_\tau(\omega,\gamma,\mathbf{r}_\tau - \mathbf{r}'_\tau) = \frac{1}{ab}\sum_{m,n=-\infty}^{\infty} \times \frac{\exp(-i\tilde{k}_{xm}(x-x') - i\tilde{k}_{yn}(y-y'))}{\tilde{k}_x^2 + \tilde{k}_y^2 - (k_0^2 - \gamma^2(\omega))}. \quad (38)$$

Here, for simplicity, we have given the GF for a rectangular cell with periods a and b, so $\tilde{k}_{xm} = k_x + 2m\pi/a$, $\tilde{k}_{yn} = k_y + 2n\pi/b$. A wave in such a PC goes in all three directions: in the longitudinal direction it is an ordinary wave, and in the transverse direction it is a Bloch wave defined by k_x and k_y. To reveal the waveguide properties in the longitudinal direction, a two-dimensional PC must have a defect. As defect may be a cylindrical cavity. Such DWs are known as photonic-crystal waveguides (PCW) of the hollow channel type in a periodic shell. If the working region falls within the band gap of a regular two-dimensional PC, such a waveguide channels the mode along the z axis. The defect can also be in the form of an optically denser inclusion. The defect can be taken into account by adding the terms corresponding to its polarization current to the two-dimensional VIE. In this case, in the case of a defect in the form of a hollow channel „, the addition of " reduces to the subtraction of the contribution from the polarization current of remote elements of the PC, and in the case of a defect in the form of an optically denser inclusion, to the addition of a contribution from the additional polarization current. This approach is algorithmically much simpler than the commonly used methods of PCW analysis [75,76]..

By analogy, we do not present the types of IDEs obtained by transferring the action of the operator ∇_τ from the kernel to the integrand. Due to the presence of a longitudinal term associated with the parameter γ, they have somewhat more cumbersome forms. Instead of integrals over the surface, they are loaded with contour integrals over the contour of the cross section. Using these equations, one can obtain functionals whose stationary values determine either the spectral parameter (transverse wave number) or the desired longitudinal wave number γ. For DW and PCW from dielectric elements, one can also formulate the IDE.with respect to only the magnetic field. Since the magnetic field does not tolerate steps at the interfaces, it is convenient, since the vector basis functions do not have to be subject to the discontinuity conditions of the normal components on the surfaces. In the work [76] the VIE for the finite cladding of a photonic-crystal waveguide was used to calculate its modes. In the paper [77] the VIE method was used to analyze the modes of a 2D PC from nanowires. VIEs for the analysis of the modes of a rectangular DW were used in the works [9,78]. Although an open rectangular DW is a simple structure, the analysis of its modes based on field decomposition in domains and stitching is quite complicated [79–89]. Mods are hybrid, having all six components. Regarding the classification of modes, there is also no uniformity. They can be classified as HE_{mn} and EH_{mn}, where m and n determine the approximate number of component variations H_z or E_z along x and y in the cross section in the case of a propagating surface mode. The oscillating field goes beyond the dielectric, so these indices are not integer (approximately integer). It is clear that the mode fields will be symmetric/antisymmetric with respect to the $x = 0$, $y = 0$ planes. In the case of $\omega\to\infty$ or $\varepsilon\to\infty$, the field does not go beyond the rectangular region, the variance tends to $\gamma(\omega) = k_0\sqrt{\varepsilon}$, and the HE_{mn} mode goes to E_{mn}, and the EH_{mn} goes to E_{mn}. In the work [79] the main two modes are classified as $HE_\perp$ and $H_\parallel$ or as even and odd with respect to the transverse electric field. In the first case, the electric field is perpendicular to the maximum side of the DW, and in the second case, it is parallel to it. The classification scheme adopted in the works [79,80] is based on the fact that with a large aspect ratio and a small difference in refractive indices in the short wavelength limit, the transverse electric field is mainly parallel to one of the transverse axes. The modes are denoted as E^y_{mn} if their electric field is parallel to the y axis in the limit, and as E^x_{mn} if their electric field is parallel to the limit axes x. The indices m and n are used to denote the number of maxima in the x and y directions, respectively. Usually, the transverse components of waveguide modes are expressed in terms of

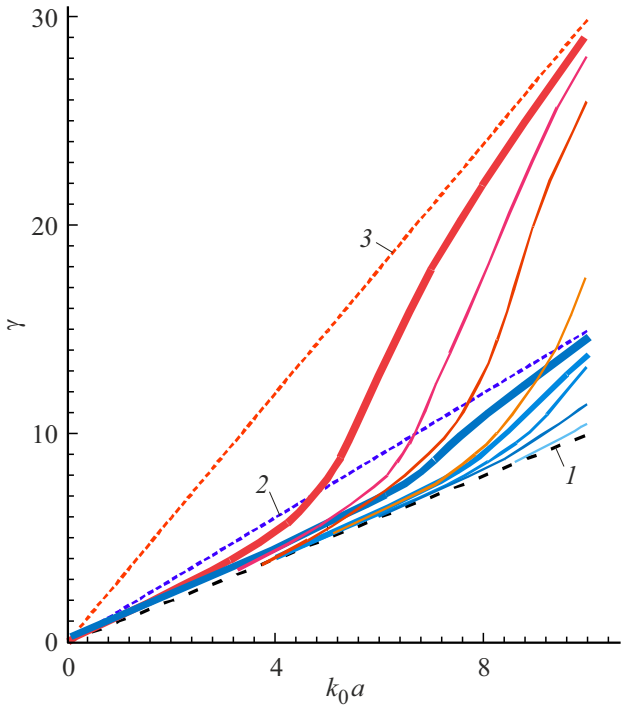

Figure 6. Dispersion of the first few HE_{mn} modes of a square DW for $\varepsilon = 2.25$ and $\varepsilon = 9.0$ DPs. The dashed line *1* denotes the low-frequency cutoff $\gamma = k_0$, the dashed line *2* — $\gamma = k_0\sqrt{2.25}$, the line it3 — $\gamma = 3k_0$. The curves for $\varepsilon = 2.25$ lie between the lines *1* and *2*, the curves for $\varepsilon = 9.0$ lie between the lines *1* and *3*. Mods without cutoff are HE_{11}. Square finite elements are used.

the longitudinal components E_z and H_z or in terms of the Hertz vectors. In the case of a rectangular DW, transverse components can be chosen instead, and this choice is not unique. The boundary conditions require consideration of all six components, i.e. modes are hybrid. In this regard, the VIE method using finite elements is convenient in that it does not require the fulfillment of boundary conditions (they are automatically satisfied when solving), which is especially convenient for complex boundaries. Comparative analysis of a number of methods for calculating the DW is given in [89].

Fig. 6 shows the results of calculating the dispersion in a square DW. The solution was obtained using square piecewise constant two-dimensional FEs. An VIE with an integrable kernel and an iterative method for determining the spectral parameter are used. $\gamma = k_0$ was assumed at the cutoff point, and for each of the frequencies above the critical one, the dispersion equation was solved by the iteration method. The iterative method is convenient because if a convergent solution is obtained at a certain frequency ω, for example, $\gamma(\omega)$, then changing the frequency by a small amount $\Delta\omega$ and using the previous solution, we obtain the value of $\gamma(\omega + \Delta\omega)$ quite accurately and quickly for the same mode at a close frequency. Thus, dispersion curves can be obtained in the region where they do not intersect. The iteration method also makes it possible to determine fast complex leaky modes.

5. Plasmon waveguides and localized plasmons

Taking the DW in the form of a rectangular region of section $a \times b$ and determining the DP by the Drude-Lorentz model, we obtain a model of a plasmonic waveguide. In the frequency region where the real part of the DP is negative, plasmon polaritons (PP) propagate in such a waveguide. Slow PPs exist in the region $\varepsilon'_m(\omega) = \mathrm{Re}(\varepsilon'_m) < -1$ where the dissipation $\varepsilon''_m(\omega)$ is not too large. This is the region of plasmon resonance. Usually, PP is considered in a layer of thickness a at $b \to \infty$ or in a structure of several layers using the matching method. Such PPs have three field components E_x, E_z and H_y. The VIE method makes it possible to consider the PP in a finite plate when all six field components are present. At low frequencies, the PP speed is close to the speed of light c, and they are weakly inflowing waves. The PP deceleration in the plasmon resonance region is the greater, the smaller the thickness a, while both forward and backward surface waves are supported [90]. Strong deceleration is obtained at thicknesses of the order of nm. The increase in deceleration is due to the interaction of surface waves on the two sides. For thin finite structures, VIEs are very convenient, since the number of FEs is small. Figure 7 shows an example of quasi-E-PP simulation for the aspect ratio $b/a = 100$ and $b/a = 10$. The algorithm was constructed as follows. The dispersion $\gamma = k_z$ for E-PP was calculated on the basis of a strict dispersion equation obtained by the matching method. This result was used as an initial approximation in the functional with respect to $\gamma = k_z$, which was obtained on the basis of the VIE, which was solved iteratively together with the calculation γ. 300 FEs were used. A similar approach to PP modeling can be applied to layered and inhomogeneous plasmonic waveguides, as well as in the case of arbitrary cross sections. At high frequencies, the metal acquires the properties of a lossy dielectric, and the considered algorithms can describe DW modes. This applies to a greater extent to semiconductor waveguides, whose plasma frequencies are much lower than those of metals. Materials for plasmonics and plasmonic waveguides are considered in the the work [91].

Methods of the VIE type are widely applied to the analysis of localized plasmons. Here, the approach is the same as for DP, but taking into account the DP of metals. Gold nanoparticles embedded in tissues and excited by a laser affect the area around them. Such methods are widely used in medicine. A significant enhancement of the field is possible with dipole, quadrupole, and other multipole excitation of several particles. A number of works are devoted to the analysis of localized plasmons by the VIE method, for example, the work [92]. Some of its results are presented in Fig. 8, 9.

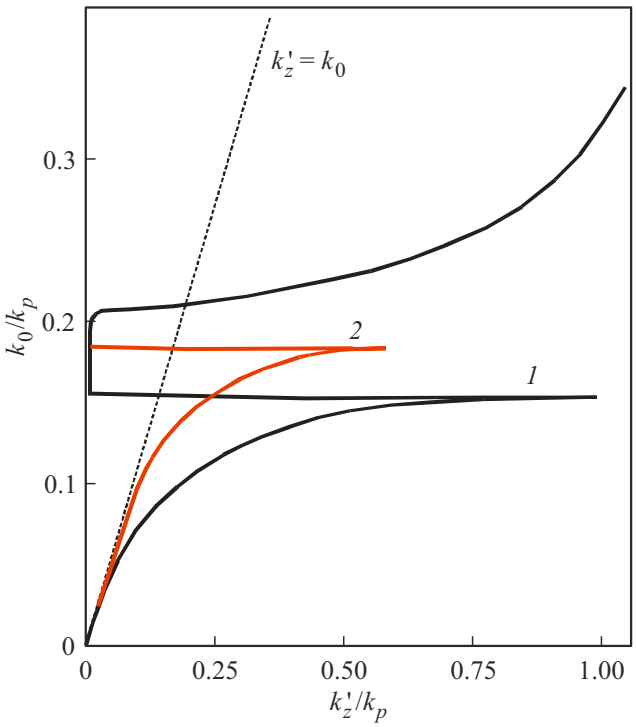

Figure 7. Plasma wavenumber normalized $k_p = \omega_p/c$ deceleration k_z' (along the abscissa) as a function of the normalized wavenumber (y-axis) for slow PP along the silver layer thicknesses 2 nm (curve *1*) and 10 nm (curve *2*). Curve *1* is constructed for $b/a = 100$, curve *2* is constructed for $b/a = 10$ nm. $\omega_p = 1.57 \cdot 10^{16}$, $\omega_c = 3.6 \cdot 10^{13}$ Hz.

6. Numerical algorithms for diffraction problems

The problems of diffraction correspond to inhomogeneous VIEs. If they are formulated with respect to electric and magnetic fields, then we introduce the bivector $\mathbf{F}^p = (\mathbf{E}, \mathbf{H})$, as well as the bivector $\mathbf{F}^0 = (\mathbf{E}^0, \mathbf{H}^0)$. The latter consists of third-party fields. They are also incident fields and can be the field of a plane wave, or, for example, the field of a dipole. The complete field is $\mathbf{F} = \mathbf{F}^0 + \mathbf{F}^p$. It is it that acts on the body, causing polarization, which is equivalent to the relation $\mathbf{F}^p(\mathbf{r}) = \hat{K}(\mathbf{r}, \mathbf{F})$, where $\hat{K}(\mathbf{r}, \mathbf{F})$ is one of the integro-differential operators defined above. Thus, the diffraction problem is defined as follows:

$$\mathbf{F}(\mathbf{r}) = \mathbf{F}^0(\mathbf{r}) + \mathbf{F}^p(\mathbf{r}) = \mathbf{F}^0(\mathbf{r}) + \hat{K}(\mathbf{r}, \mathbf{F}). \qquad (39)$$

If we use only the VIE with respect to the electric field, then all quantities $\mathbf{F}$ are replaced by $\mathbf{E}$. An approximate solution to equation (39) is $\mathbf{F}(\mathbf{r}) = \mathbf{F}^0(\mathbf{r}) + \hat{K}(\mathbf{r}, \mathbf{F}^0)$. However, further use of successive approximations may not lead to a convergent result if the parameter $\varepsilon - 1$ (or a parameter similar to it) is large. This limits the method to DP close to unity. At least it should be $0 < \varepsilon < 2$ If a singular RI with singularity extraction is used, then we get $\varepsilon < 2.5$. Therefore, equations of the type (39) are solved by numerical methods by inverting systems of linear equations of high order. Different approaches are possible here: projection-type methods of moments and Galerkin?s methods on various basis and weight functions, collocation methods, variational approaches with the construction of functionals. All of them follow from the minimization of the generalized weighted residuals [93] We have considered a body of finite volume, therefore, when using a dipole as a third-party field, the problem of excitation of such a body arises. A similar problem arises when a body is excited by a plane wave. Analytical solutions are known for the problems of excitation of an ideal dielectric sphere [68–70]. Any problem of excitation by electric and magnetic dipoles is the problem of finding the components of a tensor GF structure. For such a complete GF, all dipole orientations should be considered. In the far field zone, the field of such a delayed GF represents divergent spherical waves [28]. For a dielectric body of a complex shape, one can use the VIE with respect to the magnetic field, and as the basis functions, take its expansion in terms of spherical harmonics in the sphere describing the body, and integrate over the volume of the body. This requires numerical integration. Solving the problem of excitation by point dipoles, in principle, allows solving the problem of excitation by arbitrary sources.

The above equations are easily transformed to the form when the problem or structure is infinite in one of the coordinates. The solvability of such two-dimensional VIEs formulated with respect to electric or magnetic fields is considered in [19]. In the works [8,20,21] the solvability of singular VIEs is proved. The excitation of such structures by plane waves is usually considered. Numerical approaches to solving VIEs are studied in [10,13]. As the problems solved by the matching method, we note diffraction by round dielectric or elliptical cylinders [70]. The expansion in terms of cylindrical harmonics can be used to solve problems of diffraction on cylinders of complex cross section. Let us separately consider the problem of cylindrical structures periodically located in one of the transverse directions. This is the problem of diffraction by a PC element that is finite in one of the directions. It is also possible to consider the semi-infinite in this direction region of the FC. Such a problem can also be set for a semi-infinite 3D FC. It cannot be solved within the framework of the given VIE, since it contains infinite domains of integration. Its solution is possible taking into account a finite but large number of periods.

Diffraction by two-dimensional structures is described on the basis of a 2D scalar GF $G(\mathbf{r}_\tau - \mathbf{r}_\tau') = -(i/4)H_0^{(2)}(k_0 R)$, $R = \sqrt{(x-x')^2 + (y-y')^2}$. In this case, the plane wave diffraction problem $\mathbf{E} = \mathbf{y}_0 E_{0y} \exp(-ik_0 x)$, $\mathbf{H} = \mathbf{z}_0 \eta^{-1} E_{0y} \exp(-ik_0 x)$ TE polarizations or waves $\mathbf{E} = \mathbf{z}_0 E_{0z} \exp(-ik_0 x)$, $\mathbf{H} = -\mathbf{y}_0 \eta_0^{-1} E_{0z} \exp(-ik_0 z)$ TH-polarization on a dielectric cylinder of arbitrary cross section located at the origin along the z axis (see, for example, [94]). Figure 10 shows the directional pattern $F(\varphi/\pi) =$

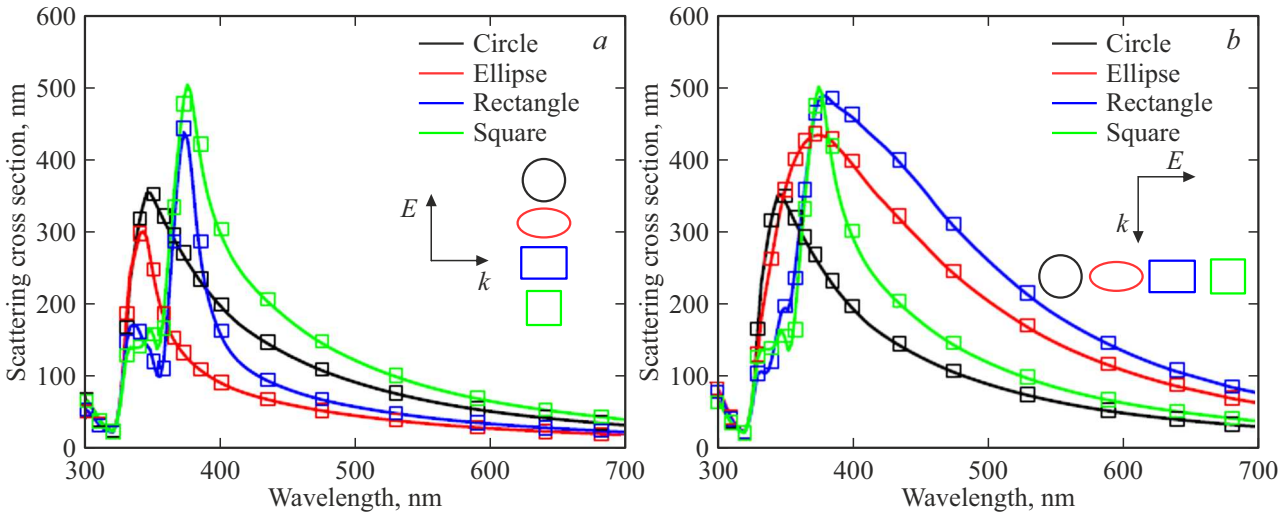

Figure 8. Scattering cross section (according to the work [92]) at angles of incidence 180° (*a*) and 90° (*b*) depending on the wavelength for cylinders of various shapes calculated by the VIE method (solid lines) and the boundary element method (square symbols). For both elliptical and rectangular cylinders, their surface plasmon resonances are redshifted, and their full widths at half maximum increase as the light incidence angle changes from 180° to 90°.

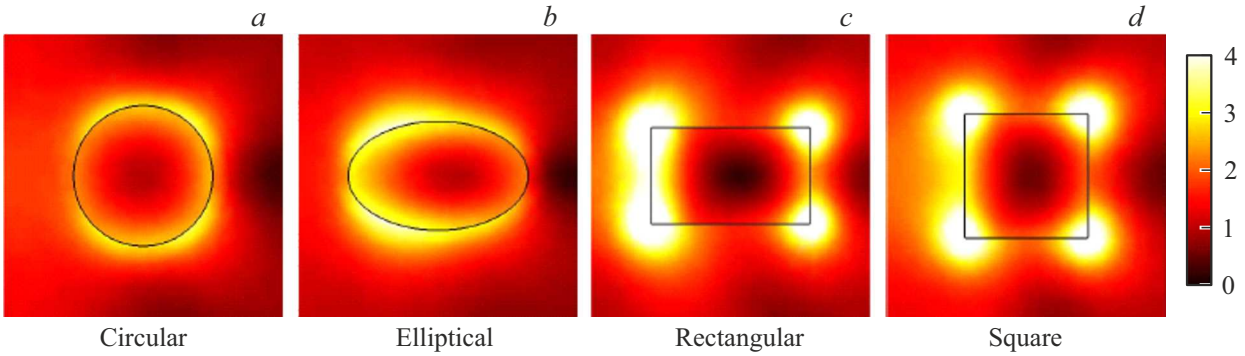

Figure 9. Normalized near field distribution of round (*a*), elliptical (*b*), rectangular (*c*), square (*d*) nanoparticles (according to [92]) at their respective resonant wavelengths when irradiated with light at an incidence angle of 180°, as shown in the insert in Fig. 8, *a*.

$|E_z(\varphi/(\varphi/\pi))/E_z(0)|^2$ of diffraction by an isotropic square dielectric cylinder with sides $2a$.

VIE-based algorithms can be built on the basis of projection or variational approaches with the same or different basis and weight functions. In the first case, we obtain methods of the Galerkin's (Bubnov-Galerkin) types and moment types, respectively, and in the second, we obtain quadratic or bilinear functionals. All of them lead to systems of linear algebraic equations, which should be solved iteratively. Direct methods are possible for bodies of small electrical dimensions. Otherwise bad conditioning occurs. It is often possible to obtain functionals for some parameters of the problem: squared resonant frequencies of the DR, reflection coefficients, input impedances, directional patterns, etc. They should be found iteratively together with the iterative solution of VIE [9,65]. In the case of bodies of small electrical size and low dielectric susceptibility $\chi = \varepsilon - 1 < 1$, when the perturbation of the field $\mathbf{E}_0$ is small, one can use perturbation theory (MSA) for the equations Lippmann-Schwinger type. This requires the calculation of multiple volume integrals, and the formulated smallness conditions for real problems are almost never satisfied. In the case of a formulation in the form of a bilinear functional with differentiable weight functions, it is convenient to transfer the action of the operator $\hat{D}$ to weight functions. In this case, to obtain matrix elements, it is necessary to integrate $G(\mathbf{r} - \mathbf{r}')$ with a weakly singular kernel.

Recently, methods related to VIE have received a lot of attention and are being used more and more widely. It should be noted the monographs [95–97], in which the main attention is paid to the mathematical problems of proving the Fredholm property of operators and the solvability of problems, as well as two monographs [98,99], which are directly related to the issues under consideration and are devoted to the transformation and solution equations of electrodynamics, including variational approaches. In the works [100–111], algorithms for solving problems for

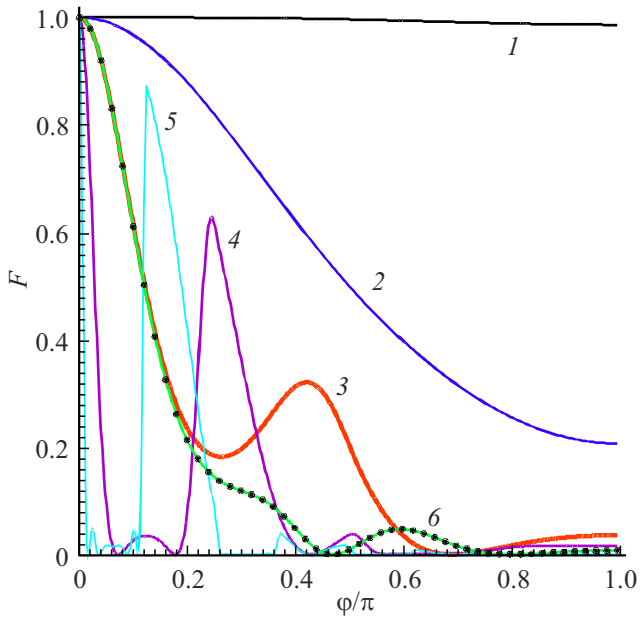

Figure 10. Directional pattern$F(\varphi/\pi) = |E_z(\varphi/\pi)/E_z(0)|^2$ of scattering of a plane wave polarized along the axis of a square dielectric cylinder for different values k_0a: *1* — 0.1, *2* — 1.0, *3, 6* — 2.0, it 4 — 4.0, *5* — 8.0. Curves *1–5* are constructed for $\varepsilon = 2.25$, curve *6* is constructed for $\varepsilon = 4$.

specific structures by the VIE method with the justification of various approximations of solutions are studied. In particular, iterative approaches to obtaining solutions are being developed [109–112].

If the spectral problem is solved, i.e., fields are found as a function of frequency, then a time-dependent non-stationary solution can be obtained by Fourier inversion. This, however, is a mathematically difficult problem, especially if one uses the numerical methods for determining spectral integrals, which are necessary for most of these problems. In a number of works, spatiotemporal VIEs [14,15,23,31,112–118] have been formulated and used. It is convenient to base them on the scalar GF $g(t-t', \mathbf{r}-\mathbf{r}')$, which is given by the inverse Fourier transform of $G(\mathbf{r}-\mathbf{r}')$ and has the form $g(t, \mathbf{r}) = (4\pi)^{-1}\delta(t-|\mathbf{r}|/c)$. For dielectric bodies, the polarization $\mathbf{P}(t, \mathbf{r}) = \mathbf{D}(t, \mathbf{r}) - \varepsilon_0\mathbf{E}(t, \mathbf{r})$, polarization current $\mathbf{J}(t, \mathbf{r}) = \partial_t\mathbf{P}(t, \mathbf{r})$ and determine the electric induction $\mathbf{D}$ through the integral connection with the field. The equations are most simply obtained in the absence of spatial dispersion. when $\mathbf{D}$ is related to $\mathbf{E}$ by an integral operator with kernel $\varepsilon_0\varepsilon(t-t', \mathbf{r})$, where $\varepsilon(t, \mathbf{r})$ is the inverse transformation from $\varepsilon(\omega, \mathbf{r})$, and the integration is over t'. The kernel satisfies the principle of causality: $\varepsilon(t, \mathbf{r}) = 0$ for $t > 0$, which means that the contribution to the polarization is only from electric fields at previous times. Accounting for spatial dispersion leads to the fact that the connection becomes nonlocal with the kernel $\varepsilon_0\varepsilon(t-t', \mathbf{r}-\mathbf{r}')$ and is determined by space and time integrals. In the spatial integral, one should take into account only those points in the neighborhood of the point $\mathbf{r}$ for which $|\mathbf{r}-\mathbf{r}'| < c(t-t')$, i.e. for which the perturbation has time to reach the point of observation. In the resulting VIEs, the Heaviside function $\chi(t-t'-|\mathbf{r}-\mathbf{r}'|/c)$ appears, indicating that the contribution to the field at some point at a given moment $\chi(t-t'-|\mathbf{r}-\mathbf{r}'|/c)$ are introduced only by those points of the body, at the moment t', the perturbation from which manages to reach the speed of light c. The simplest non-stationary equations arise under bonds local in time and space $\mathbf{D}(\mathbf{r}, t) = \varepsilon_0\varepsilon(\mathbf{r})\mathbf{E}(\mathbf{r}, t)$. However, such connections are possible when the DP dispersion can be neglected, which is usually the case for a very low-frequency spectrum of the wave packet.

As noted, a metallic body can be described by a DP. But when in the main part of the spectrum the penetration depth is negligibly small compared to the dimensions of the body, it is convenient to describe it by the surface current density $\mathbf{j}$. It should also be introduced in the case of graphene and similar two-dimensional structures in the presence of dielectric bodies. In this case, surface integrals additionally appear, and the equations become combined volume-surface equations. The introduction and use of such equations has recently been the subject of many works, for example [118–120]. Equations are considered both with respect to fields and with respect to potentials. Since the potentials can be introduced in different ways, there can also be many possible equations. Various approximations are considered both in volume and on the surface. Each equation can be associated with several algorithms. They are more complicated for the combined volume-surface equations, since they also require the definition of the surface current $\mathbf{j}$. The latter satisfies the continuity equation, therefore, when transforming the surface integral with the transfer of the divergence operator to it, it is necessary to determine the surface charge density $\sigma(\omega, \mathbf{r}_s) = i\omega^{-1}\nabla_s \cdot \mathbf{j}(\omega, \mathbf{r}_s)$. The index s here means the radius vector tangent to the surface and the surface divergence. The impedance boundary condition $\mathbf{E}(\omega, \mathbf{r}_s) = Z_s(\mathbf{r}_s)\mathbf{j}(\omega, \mathbf{r}_s)$, which is an additional condition for determining $\mathbf{j}$. Let?s emphasize once again that the solution of the VIE inside the body automatically implies the boundary conditions for the field $\mathbf{E}$ at the boundary of the body and the radiation conditions at infinity. In the English-language literature, the following classifications of equations are used: IEs relative to electric field (EFIE),magnetic field (MFIE),relative to mixed potentials (MPIE),volume-surface IEs (VSIE), hybrid IEs, etc. The combination of surface and volumetric IEs makes it possible to analyze all possible structures encountered in problems of electrodynamics and optics.

7. Calculation of matrix elements

Matrix elements for simple configurations (cubes, etc.) can be constructed using Fourier bases such as sines and cosines. However, a more general approach applicable to bodies of complex shape is based on FEs. This requires discretization of the volume of bodies. For VIEs, apparently,

the most convenient is cubic discretization with a cube size of Δ. The simplest finite elements are piecewise constant. They are built on a single cube and require the integrability of the kernels. Smooth FEs usually require 3 or 5 digitalization points for each of their variables, i.e. 27 or 125 such cubes per volumetric FE that is tied to the central node. Various approximations of FE by polynomials are also possible. Smooth (differentiable) FEs lead to complex algorithms, especially for complex interfaces. Quadrature formulas for calculating integrals are more convenient. Since the integrals in the matrix element are sixfold in two space variables $\mathbf{r}$ and $\mathbf{r}'$, it is convenient to shift the points of nodes $\mathbf{r}_j, \mathbf{r}'_j$, for example, by $\Delta/2$ for each of the variables. For kernels in the coordinate representation, it is convenient to assume that the integration elements are constant. In this case, the matrix elements are calculated as simply as possible, and the diagonal elements are finite. In the case of VIE with a distinguished non-integral term, the diagonal elements should be set to zero. For kernels in the spatial-spectral representation, the dependence on coordinates has the form $\exp(-i(\mathbf{r}'))$. Integration with this function on biased FEs leads to $f_{jj'}(\mathbf{k}) = f(k_x, x_j - x'_{j''}) f(k_y, y_j - y'_{j''}) f(k_z, z_j - z'_{j''})$, where $f(k, x) = \Delta \exp(-ikx) \sin c(k\Delta)$, where the function $\sin c(x) = \sin(x)/x$ is denoted. Therefore, matrix elements are defined as integrals in $\mathbf{k}$-space of $\Gamma_{\alpha\beta}(\mathbf{k}) f_{jj'}(\mathbf{k})$, where $\Gamma_{\alpha\beta}(\mathbf{k})$ are spectral parts of tensor GFs. These integrals usually converge slowly, so significant efforts in obtaining algorithms can be expended on improving the convergence of the integrals. For weakly singular kernels with singularities $|\mathbf{r} - \mathbf{r}'|^{-\alpha}$, $\alpha = 1, 2$, when calculating the diagonal matrix elements, it is convenient to replace the cubic cell with a solid sphere of equivalent volume: $\Delta^3 = 4\pi r_0^3/3$. Then the integration in the approximation of the constancy of the functions taken in the cell is performed analytically:

$$\int\limits_{|\mathbf{r}-\mathbf{r}'|^2 \le r_0^2} |\mathbf{r} - \mathbf{r}'|^{-\alpha} d^3r d^3r' = 4\pi\Delta^3 r^{2-\alpha} dr$$

$$= 4\pi\Delta^{6-\alpha} (3/(4\pi))^{3-\alpha/3}/(3-\alpha).$$

Other approximations can also be used to calculate matrix elements. In the DR problem in Fig. 1–3, due to azimuthal symmetry, the kernel has a weak singularity, and quadrature formulas are used. Note that here the VIE for E_φ is the same as for the vector-potential component. In the DW problem, we used an VIE with an integrable kernel and shifted FEs. the problem of variance in a FC, an VIE with a distinguished non-integral term and a periodically translated GF $G(k, \mathbf{r} - \mathbf{r}')$ is used. In the problem of the directional pattern, the Hankel function [28] and discretization on shifted grids were used as a scalar GF.

8. Conclusion

The review considers 3D and 2D VIEs in the frequency domain and presents their types, which describe free oscillations and waves in DR, DW, and in fibers of arbitrary shape and anisotropy, including taking into account inhomogeneous and nonlinear properties, as well as diffraction by dielectric and magnetic bodies. Based on such equations, plasmonic waveguides and localized plasmons can be analyzed. A review of publications where the VIE method is used, is given. The review does not claim to be complete coverage of the material. As for the analysis of DRs with nonlinear properties, in a strong field this is a purely non-stationary problem: as the field is emitted from the DR volume, the intensity decreases and the resonant frequency changes. The nonstationary approach should also be used for a DW with a nonlinear dielectric, since the nonlinearity changes the spectral composition of the wave packet, and it is very difficult to propagate along the DW, especially if there is a strong frequency dispersion and inhomogeneous (selective) absorption. This problem is associated with the excitation of DWs and fiber waveguides by high-power laser beams when waves are multiplied and a supercontinuum is generated. Accordingly, one should consider the finite spectrum of waves in the wave packet and the non-stationary problem. If, nevertheless, the spectrum is narrow, a single-frequency approximation is possible. In this review, we brushed over the problem of non-stationary problems. It is possible to formulate non-stationary equations for waveguide structures as well. The review did not cover numerical methods and justifications for solving hypersingular integral equations. For 1D equations, this term was introduced by J. Hadamard, and for the first time he considered surface IEs for electrodynamics in 1949 A. Maue [121]. These equations have not been directly used for numerical solution for a long time, and only relatively recently have algorithms been applied to them. In the 1D case, the equations describe thin dipole antennas. For surface hypersingular IEs, the methods are based on the representation of fields as a finite part of the integral in the sense of the Hadamard value as the observation point tends to the surface. Theoretical approaches are closely related to the theory of pseudodifferential operators [33–35,122]. The reader who is interested in these questions can be recommended literature [122–125].

The numerical results presented in the review for a cylindrical DR, rectangular DW, dispersion in a PC and in a plasmonic waveguide, and diffraction by a dielectric structure were obtained by the author. As regards the efficiency and accuracy of the VIE method, it can be estimated based on the calculation of the resonant frequencies of the DR, which can be quite accurately measured. In particular, Fig. 3 demonstrates the convergence depending on the number of partitions (nodes) along each of the two coordinates. The number of test functions (matrix order) here is N^2. When smooth FEs are used, the dimension of the problem is reduced by about 4 times, i.e.,

to achieve the same accuracy, 4 times fewer basis functions are needed. However, such FEs lead to the complexity of the algorithm. The calculated results for eigenfrequencies are about 1−1.5% lower than the data from the paper [4], where the experimental results are also presented. The experimental results are 1−2% higher than the calculations in [4]. For curves (*2, 3*) in Fig. 3 refinement by Aitken's method gives the frequency $f = 5.23752\angle$ GHz, while in [4] the frequency $f = 5.289$ GHz. On the other hand, the solution of a self-adjoint problem with a linear occurrence of the eigenvalue k_0^{-2} (i.e., for FG at $k_0 = 0$) by the considered methods gives the values , almost identical to [4]. From this we can conclude that the results [4] were obtained with a defect. The frequencies H_{011} of oscillations for the considered form of DR are approximately one and a half times, and the quality factors are more than an order of magnitude higher than for the lowest type $H_{01\delta}$ oscillations, since in the first case the quality factor is associated with magnetic dipole radiation, in the second is associated with magnetic quadrupole. Calculations show that the achievement of high quality factors at the lowest modes requires the use of $\varepsilon > 40$ values at a negligibly small loss tangent. Qualitatively, the total quality factor can be estimated through the radiative one from the relation $Q^{-1} = Q_R^{\text{l}} + \varepsilon''/\varepsilon'$, however, the method allows it to be calculated using the complex DP. If there is a strong frequency dispersion of the DP, then the resulting equations always need an iterative solution. Indeed, the parameter $k_0 = \omega/c$ enters the equations non-linearly (directly and through the GF), just like the frequency. It is necessary to freeze the frequency in the DP, obtain the resonant frequency, correct the DP, and continue the process until convergence.

The VIE method as a research tool occupies a certain place in computational electrodynamics. However, in our opinion, it is underestimated in terms of its capabilities, although the number of publications using it is growing. It can be applied in integrated optics, photonics, plasmonics, for the analysis and homogenization of PCs (see, for example, [16–18]), as well as for 1D, 2D, and 3D stationary and non-stationary problems of quantum mechanics [15]. In addition to stationary and non-stationary problems of electrodynamics, it was also applied to problems of magnetostatics with nonlinear magnetic structures [126–129], to problems of mechanics, acoustics [118] and to a number of other problems.

Funding

The study was performed with the support of the Ministry of Education and Science of Russia as part of the Government Task (project № FSRR-2020-0004).

Conflict of interest

The author declares that he has no conflict of interest.

References

[1] N.A. Khizhnyak. ZhTF,**28** (7), 1592−1604 (1958) (in Russian).
[2] C. Müller. *Foundation of the mathematical theory of electromagnetic waves* (Berlin-Heidelberg, Springer-Verlag, 1969).
[3] *Computational methods in electrodynamics*. Ed. R. Mittra (Mir, Moscow, 1977). [*Computer techniques for electromagnetics* (in Russian) Ed. R. Mittra (Pergamon Press, Oxford, N.Y., Toronto, Sydney, Braunschweig, 1973)].
[4] L.B. Goldberg, V.V. Penzyakov. Radiotekhnika i elektronika, **27**, 9 1735–1740 (1982).(in Russian).
[5] E.N. Vasiliev. *Vozbuzhdeniye tel vrashcheniya* (Radio i svyaz', M., 1987).(in Russian).
[6] N.A. Khizhnyak. *Integral'nyye uravneniya makroskopicheskoy elektrodinamiki* (Naukova dumka, Kiyev, 1986)..(in Russian)
[7] V.I. Dmitriyev, Ye.V. Zakharov. *Integral'nyye uravneniya v krayevykh zadachakh elektrodinamiki* (Izd-vo MGU, M., 1987).(in Russian)
[8] A.B. Samokhin. *Integral'nyye uravneniya i iteratsionnyye metody v elektromagnitnom rasseyanii* (Radio i svyaz', M., 1998). (in Russian)
[9] M.V. Davidovich. *Iteratsionnyye metody resheniya zadach elektrodinamiki* (Izd-vo Sarat. un-ta, Saratov, 2014) .(in Russian).
[10] M.M. Botha. J. Computational Phys., **218** (1), 141–158 (2006). DOI: 10.1016/j.jcp.2006.02.004.
[11] M.I. Sancer, K. Sertel, J.L. Volakis, P. Van Alstine. IEEE Trans., **AP-54** (5), 1488–1495 (2006). DOI: 10.1109/TAP.2006.874316.
[12] J. Markkanen, C.-C. Lu, X. Cao, P. Ylä-Oijala. IEEE Trans., **AP-60** (5), 2367–2374 (2012). DOI: 10.1109/TAP.2012.2189704.
[13] J. Lee, M. Han. Mathematics, **8** (11), 1866(1–26) (2020). DOI:10.3390/math8111866
[14] M.V. Davidovich. Izvestiya Saratovskogo universiteta Novaya Seriya. (in Russian). Seriya: Fizika, **21** (2), 116–132 (2021). [Izvestiya of Saratov University. (in Russian). New Series. Series: Physics, **21** (2), 116–132 (2021). https://doi.org/10.18500/1817-3020-2021-21-2-116-132].
[15] M.V. Davidovich. Pis'ma v ZhETF, **108** (5), 299–326 (2018). [M.V. Davidovich. Jetp. Lett., **110** (7), 472-480. DOI: 10.1134/S0370274X19190068].
[16] M.V. Davidovich. Pis'ma v ZhETF, **108** (5), 299–326 (2018). [M.V. Davidovich.(in Russian) Pis'ma v ZhETF,, **108** (5), 279–286 (2018).(in Russian) DOI: 10.1134/S0370274X18170010].
[17] M.V. Davidovich. ZhETF, **154** (7), 5–25 (2018). [M.V. Davidovich .(in Russian) ZhETF, **127** (1), 1–19 (2018) (in Russian) DOI: 10.1134/S1063776118070178].
[18] M.V. Davidovich. UFN, **189** (12), 1250–1284 (2019). [M.V. Davidovich. Phys. Usp., **62** (12), 1173–1207 (2019) (in Russian) DOI: 10.3367/UFNr.2019.08.038643].
[19] M. Costabel, E. Darrigrand, H. Sakly. Computers & Mathematics with Applications, **70** (8), 2087–2101 (2015). DOI: 10.1016/j.camwa.2015.08.026
[20] A.B. Samokhin. Differentsial'nyye uravneniya, **50** (9), 1215–1230 (2014) (in Russian)
[21] A.B. Samokhin, A.S. Samokhina. Diff. uravneniya, **52** (9), 1221–1230 (2016). [A. Samokhin, A.S. Samokhina. Differen-

tial Equations, **52** (9), 1178–1187 (2016)].
[22] A.B. Samokhin, A.S. Samokhina, Yu.V. Shestopalov. Differentsial'nyye uravneniya, **54** (9), 1251–1261 (2018). [A. Samokhin, A.S. Samokhina, Yu.V. Shestopalov. Differential Equations, **54** (9), 1225–1235 (2018)].
[23] A.B. Samokhin, A.S. Samokhina, K. Kobayashi. Differentsial'nyye uravneniya, **55** (9), 1293–1300 (2019). [A.B. Samokhin, A.S. Samokhina, K. Kobayashi. Differential Equations, **55** (9), 1250–1257 (2019)].
[24] A.B. Samokhin. ZhVMMF, **32** (5), 772–787 (1992). [A.B. Samokhin. Computational Mathematics and Matematical Physics, **32** (5), 673–686 (1992)].
[25] A.B. Samokhin. Differentsial'nyye uravneniya, **30** (12), 2162–2174 (1994). (1994). [A.B. Samokhin Differ. Equ., **30** (12), 1987–1997 (1994)].
[26] A.B. Samokhin. Differentsial'nyye uravneniya, **31** (9), 1588–1590 (1995). (1994). [A.B. Samokhin Differ. Equ., **31** (9), 1548–1551 (1995)].
[27] A.B. Samokhin. Differ. Uravneniya, **37** (10), 1357–1363 (2001). [A.B. Samokhin. Differ. Equ., **37** (10), 1427–1434 (2001)].
[28] G.T. Markov, A.F. Chaplin. *Vozbuzhdenie elektromagnitnykh voln* (Radio i svyaz, M., 1983) (in Russian).
[29] M.V. Davidovich. ZhETF, **159** (2), 195–215 (2021). [M.V. Davidovich. JETP, **32** (2), 159–176 (2021). DOI: 10.1134/S1063776121020102].
[30] L.A. Vainshtein. *Elektromagnitnye volny* (Radio i Svyaz', Moscow, 1988) (in Russian).
[31] M.V. Davidovich. Radiotekhnika i elektronika, **46**, 11 (1285) (in Russian).
[32] T. Søndergaard. Phys. Rev. B, **66**, 155309 (2002). DOI: 10.1103/PhysRevB.66.155309.
[33] G.E. Eskin. *Krayevyye zadachi dlya ellipticheskikh psevdodifferentsial'nykh uravneniy* (Nauka, M., 1973 (in Russian).
[34] M. Teylor. *Psevdodifferentsial'nyye operatory* (Mir, M., 1985). [M. Taylor. *Pseudo differential operators* (Springer, 1974)].
[35] A.S. Il'inskiy, YU.G. Smirnov. *Difraktsiya elektromagnitnykh voln na provodyashchikh ekranakh* (*psevdodifferentsial'nyye operatory v zadachakh difraktsii*) (IPRZhR, M., 1996 (in Russian).
[36] G.A. Ilyinsky. Radiotekhnika i elektronika, **50** (2), 134–139 (2005). (in Russian).
.S. Ilyinsky, V.V. Kravtsov, A.G. Sveshnikov. *Mathematical models of electrodynamics* (Vysshaya Shkola, Moscow, 1991) (in Russian).
[38] S.G. Mikhlin. Uspekhi Mat. Nauk, **3** (3), 29–112 (1948).
S.G. Mikhlin. *Mnogomernyye singulyarnyye integraly i integral'nyye uravneniya* (GIFML, M., 1962). (in Russian).
[40] M.V. Davidovich. Radiotekhnika, **10**, 57−62 (2014) (in Russian).
[41] A.N. Tikhonov, A.A. Samarsky. *Uravneniya matematicheskoy fiziki* (Nauka, M., 1977), p. 50 (in Russian)
[42] G. Korn, T. Korn. *Spravochnik po matematike dlya nauchnykh rabotnikov i inzhenerov* (Nauka, M., 1973).
[43] G.T. Markov, B.A. Panchenko. Izvestiya Vuzov. SSSR. Radiotekhnika, **7** (1), 34–41 (1964).
[44] M.V. Davidovich. ZhTF, **83** (7), 135–145 (2013). [M.V. Davidovich. Technical Physics, **58** (7), 1061–1072 (2013). DOI: 10.1134/S1063784213070049].
[45] J. Schwinger, L. DeRaad, K. Milton. Casimir effect in dielectrics. Annals of Physics, **115** (1), 676–698 (1978).
[46] N.K. Das, D.M. Pozar. IEEE Trans., **MTT-35** (3), 326–333 (1987). DOI: 10.1109/TMTT.1987.1133646.
[47] K.A. Michalski, J.R. Mosig. EEE Trans., **AP-45** (3), 508–519 (1997). DOI: 10.1109/8.558666.
[48] K. Li. In: IEEE Antennas and Propagation Society International Symposium & USNC/URSI National Radio Science Meeting. 1999 Digest, vol. 2, p. 1266–1269. DOI: 10.1109/APS.1999.789544
[49] T. Yuan, M. Zhang, L.-W. Li, L. Zhang, M.S. Leong. In: IEEE 2004 Asia-Pacific Radio Science Conference, p. 277–279. DOI: 10.1109/APRASC.2004.1422524
[50] T.F. Elshafiey, J.T. Aberle. IEEE Trans., **MTT-54** (2), 513–521 (2006). DOI: 10.1109/TMTT.2005.862706
[51] M.V. Davidovich. In: *Modeling in applied electromagnetics and electronics*, Saratov University Press, Saratov, **7**, 30–38 (2006).
[52] L.TS. Dao. *Matematicheskiye metody v fizike* (Mir, M., 1965) (in Russian)
N.M. G?nther. *Potential Theory and Its Applications to the Main Problems of Mathematical Physics* (GITTL, Moscow, 1953).
[54] A.N. Tikhonov, A.A. Samarsky. *Teoriya potentsiala i yeye primeneniya k osnovnym zadacham matematicheskoy fiziki* (GITTL, M., 1953) (in Russian).
[55] *Dielektricheskiye rezonatory*,Ed. M.E. Ilchenko (Radio and communication, M., 1989) (in Russian).
[56] D. Kajfez, P. Guillon (eds.). *Dielectric Resonators* (Artech House, Nonvood, MA, 1986).
[57] J. Van Bladel. IEEE Trans., **MTT-23** (2), 199–208 (1975). DOI: 10.1109/TMTT.1975.1128528.
[58] M. Gastine, L. Courtois, J.L. Dormann. IEEE Trans., **MTT-15** (12), 694–700 (1967).
DOI: 10.1109/GMTT.1967.1122589.
[59] P. Guillon, Y. Garault. IEEE Trans., **MTT-25** (11), 916–922 (1977). DOI: 10.1109/TMTT.1977.1129241
[60] J. Ruiz, M.J. Nufez, A. Navarro, E. Martin. IEEE Trans., **MTT-37** (11), 1814–1816 (1989). DOI: 10.1109/22.41050.
[61] J. Krupka. IEEE Trans., **MTT-33** (3), 274–277 (1985). DOI: 10.1109/TMTT.1985.1132999.
[62] R.K. Mongia, A. Atipiboon, M. Cuhaci, D. Roscoe. Electron. Lett., **30** (17), 1361–1362 (1994).
DOI: 10.1049/el:19940968.
[63] Y. Liu, S. Safavi-Naeini, S.K. Chaudhuri, R. Sabry. IEEE Trans., **AP-52** (1), 327–332 (2004).
DOI: 10.1109/TAP.2003.822424.
[64] S.Y. Ke, Y.T. Cheng. IEEEE Trans., **MTT-49** (3), 571–574 (2001). DOI: 10.1109/22.910568.
[65] M.V. Davidovich, Yu.V. Stefyuk. Izvestiya Vuzov. Radiofiyika **53** (4), 296–309 (2010). [M.V. Davidovich, Yu.V. Stefyuk. Radiophysics and Quantum Electronics, **53** (4), 268–279 (2010)].
[66] M.V. Davidovich. Izvestiya Saratovskogo universiteta Novaya Seriya. (in Russian). Seriya Fizika, **8** (1), 3–14 (2008) (in Russian)
[67] M.V. Davidovich, A.K. Kobets, K.A. Sayapin. Fizika volnovykh protsessov i radiotekhnicheskiye sistemy, **24** (3), 18–27 (2021) (in Russian). DOI: 10.18469/1810-3189.2021.24.3.18-27.
[68] G. Mie. Leipzig Ann. Phys., **330**, 377–445 (1908). http://www.elch.chem.msu.ru/rus/mfti/mie1908.pdf.
[69] M. Born, E. Vol'f. *Osnovy optiki* (Nauka, M., 1973). [M. Born, E. Volf. *Principles of optics* (Pergamon Press, Oxford, London, Edinburgh, N.Y., Paris, Frankfurt, 1968].

[70] A. Zommerfel'd. *Differentsial'nyye uravneniya v chastnykh proizvodnykh fiziki* (IL, Moskva, 1950, 458 s.). [A. Sommerfeld. *Partielle Differential Gleichungen der Physik* (Zweite Auflage, Leipzig, 1948)].
[71] G.A. Grinberg. *Nekotoryye voprosy matematicheskoy teorii elektricheskikh i magnitnykh yavleniy* (Izd-vo AN SSSR, M.-L., 1948)
[72] L.D. Gol'dshteyn, N.V. Zernov. *Elektromagnitnyye polya* (Sov. radio, M., 1971) (in Russian).
[73] L.A. Vaynshteyn. *Otkrytyye rezonatory i otkrytyye volnovody* (Sov. radio, M., 1966) (in Russian).
V.V. Klimov. *Nanoplazmonika* (Fizmatlit, M., 2010).
[75] YA.O. Shuyupova, V.V. Kotlyar. (in Russian). Komp'yuternaya optika, **33** (1), 27 (36) (in Russian).
[76] M.V. Davidovich, Yu.V. Stefyuk. Optika i spektroskopiya, **109** (4), 643–655 (2010). [M.V. Davidovich, Yu.V. Stefyuk Optics and Spectroscopy, **109** (4), 596–607 (2010)].
[77] M.V. Davidovich, I.S. Nefedov. ZhETF, **145** (5), 771–786 (2014). [M.V. Davidovich. JETP, **118** (5), 673–686. DOI: 10.1134/S1063776114040104].
[78] M.V. Davidovich. In: *17th International Conference on Microwaves, Radar and Wireless Communications* (MIKON, 2008), p. 19–21.
[79] W. Schlosser, H.G. Unger. *Partially filled waveguides and surface waveguides of rectangular cross section. In Advances in Microwaves, Academic* (New York, 1966), p. 319–387.
[80] J. Goell. Bell Syst. Tech. J., **48**, 2133–2160 (1969). https://ieeexplore.ieee.org/document/6769760.
[81] E.A.J. Marcatili. Bell System. Tech. J., **48**, 2071–2102 (1969). https://ieeexplore.ieee.org/document/6769758.
[82] R.M. Knox, P.P. Toulios. In: Proc. MRI Symp. Submillimeter Waves, 1070, p. 497–516.
[83] S. Akiba, H.A. Haus. Appl. Opt., **21**, 804–808 (1982). https://pubmed.ncbi.nlm.nih.gov/20372543/.
[84] A. Kumar, K. Thyayarajan, A.K. Ghatak. Opt. Lett., **8**, 63–65 (1983). https://pubmed.ncbi.nlm.nih.gov/19714136/.
[85] M.D. Feit, J.A. Fleck. Appl. Opt., **19**, 1154–1164 (1980). https://pubmed.ncbi.nlm.nih.gov/20221001/.
[86] C. Yeh., K. Ha, S.B. Dong, W.P. Brown. Appl. Opt., **18**, 1490–1504 (1979). https://pubmed.ncbi.nlm.nih.gov/20212884/.
[87] A.W. Snyder, W.R. Young. J. Opt. Soc. Amer., **68**, 297–309 (1978). https://opg.optica.org/josa/abstract.cfm?uri=josa-68-3-297.
[88] H. Kogeljiik, V. Ramaswamy. Appl. Opt., **8**, 1857–1862 (1974). https://opg.optica.org/ao/abstract.cfm?uri=ao-13-8-1857.
[89] S.B. Raevsky, A.Yu. Sedakov, A.A. Titarenko. Fizika volnovykh protsessov i radiotekhnicheskiye sistemy, **19** (3), 45–48 (2016) (in Russian).
[90] M.V. Davidovich. Kvantovaya elektronika, **47** (6), 567–579 (2017). [M.V. Davidovich. Quantum electronics, **47** (6), 567–579 (2017). DOI: 10.1070/QEL16272].
[91] R. Yang, Z. Lu. Int. J. Opt. 2012(1). Article ID 258013, 1–12. DOI: 10.1155/2012/258013.
[92] W.-B. Ewe, H.-S. Chu, E-P. Li. Opt. Exp., **15** (26), 18200(1–8) (2008). DOI: 10.1364/OE.15.018200.
[93] K. Brebbiya, ZH. Telles, L. Vroubel. *Metody granichnykh elementov* (Mir, M., 1987).
[94] S. Solimeno, B. Krozin'yani, P. Di Porto. *Difraktsiya i volnovodnoye rasprostraneniye opticheskogo izlucheniya* (Mir, M., 1989), 664 s. [S. Solimeno, B. Crosignani, P. Di Porto. *Diffraction and Confinement of Optical Radiation* (Academic, Orlando, 1986)].
[95] R. Kress. *Linear Integral Equations*. Applied Mathematical Sciences, vol. 82 (Springer-Verlag, New-York, 1989).
A.B. Samokhin. *Ob"yemnyye singulyarnyye integral'nyye uravneniya elektrodinamiki* (Tekhnosfera, M., 2021(in Russian)
[97] Ye.M. Karchevskiy, A.G. Frolov. *Dvumernyye singulyarnyye i slabo singulyarnyye integral'nyye uravneniya v teorii dielektricheskikh volnovodov* (Izd-vo Kazan. un-ta, Kazan', 2018)(in Russian)
V.V. Nikol'skiy. *Variatsionnyye metody dlya vnutrennikh zadach elektrodinamiki* (Nauka, M., 1967)..(in Russian)
E.V. Zakharov, Yu.V. Pimenov. *Chislennyy analiz difraktsii radiovoln* (Radio i svyaz', M., 1982).(in Russian).
[100] K. Katsinos, G.P. Zouros. In: 2021 IEEE 15th European Conference on Antennas and Propagation (EuCAP), p. 1–5. DOI:10.23919/EuCAP51087.2021.9411267.
[101] S. Tao, R.A. Chen. IEEE Antennas and Wireless Propagation Lett., **13**, 627–630 (2014).
DOI: 10.1109/LAWP.2014.2312736.
[102] A.M. Lerer, I.V. Donets, G.A. Kalinchenko, P.V. Makhno. Photonics Research, **2** (1), 31–37. (2014).
DOI: 10.1364/PRJ.2.000031.
[103] A.F. Peterson. In: IEEE 2013 USNC-URSI Radio Science Meeting (Joint with AP-S Symposium), p. 159. DOI: 10.1109/USNC-URSI.2013.6715465.
[104] A. Boag, V. Lomakin. IEEE Antennas and Wireless Propagation Letters, **11**, 568–1571 (2012).
DOI: 10.1109/LAWP.2012.2236294.
[105] M.Yu. Medvedik, Yu.G. Smirnov. Izv. VUZOV. Povolzhskiy region. Fiz.-Mat. Nauki, **4**, 54–69 (2009).(in Russian). URL: https://rucont.ru/efd/269849 (reference date: June 08, 2022).
[106] Yu.G. Smirnov, A.A. Tsupak. ZhVMMF **44** (12), 2252–2267 (2004).
[107] A.A. Tsupak. In: *Proceedings of the Karlstad Workshop on Applied Mathematics (KWAM'03)*, 7–11 September (Karlstad, Sweden, 2003).
[108] Yu.G. Smirnov, A.A. Tsupak. Izvestiya vysshikh uchebnykh zavedeniy. Povolzhskiy region. Yestestvennyye nauki, **2**, 31–43 (2003).
[109] A. Samokhin, Y. Shestopalov, K. Kobayashi. Appl. Math. Comput., **222**, 107–122 (2013).
DOI: 10.1134/S0012266114090079.
[110] T. Deng, X. Liu. In: IEEE 1995 Antennas and Propagation Society International Symposium Digest, p. 1573–1576. DOI: 10.1109/APS.1995.530878.
[111] D.E. Livesay, K.M. Chen. In: S-MTT International Microwave Symposium Digest, 1974, p. 35–37. DOI: 10.1109/MWSYM.1974.1123471.
[112] M.V. Davidovich. Radiotekhnika i elektronika, **46**, 10 1198–1205 (2001).(in Russian).
[113] M.V. Davidovich. ZhTF, **76** (1), 13–23 (2006). [M.V. Davidovich. Technical Physics, **51** (1), 11–21. DOI: 10.1134/S1063784206010026].
[114] Y. Liu, A. Al-Jarro, H. Bağcı, E. Michielssen. In: IEEE 2013 USNC-URSI Radio Science Meeting (Joint with AP-S Symposium), p. 49. DOI: 10.1109/USNC-URSI.2013.6715355.
[115] H.A. Ülkü, S.B. Sayed, H. Bagci. In: IEEE 2014 USNC-URSI Radio Science Meeting, p. 39. DOI: 10.1109/USNC-URSI.2014.6955421.
[116] Y. Liu, A. Al-Jarro, H. Bağcı, E. Michielssen. IEEE Trans., **AP-64** (6), 2378–2388 (2016).

DOI: 10.1109/TAP.2016.2546964.
[117] A.B. Samokhin, A.S. Samokhina, I.A. Yurchenkov. Differentsial'nyye uravneniya, **57** (9), 1273–1279 (2021). [A.B. Samokhin, A.S. Samokhina. Differential Equations, **57**, 1249–1255 (2021). DOI: 10.1134/S0012266121090123].
[118] B.G. Ward. IEEE Trans., **AP-69** (3), 1545–1552 (2021). DOI: 10.1109/TAP.2020.3026418.
[119] X. Li, L. Lei, Y. Chen, M. Jiang, J. Hu. In: 2018 IEEE International Symposium on Antennas and Propagation & USNC/URSI National Radio Science Meeting, p. 1–3. DOI: 10.1109/ISAPE.2018.8634188.
[120] M.V. Davidovich, S.G. Suchkov, N.A. Bushuev. Izv. vuzov. PND, **23** (1), 76–91 (2015).
[121] A.W. Maue. Zeitschrift für Physik, **26**, 601–618 (1949). DOI: 10.1007/BF01328780.
[122] I. Lifanov, L. Poltavskii, G. Vainikko. Hypersingular Integral Equations and Their Applications (CHAPMAN & HALL/CRC A CRC Press Company, Boca Raton, London, New York, Washington, 2003), 395 p. DOI: 10.1201/9780203402160.
[123] A.G. Davydov, E.V. Zakharov, Yu.V. Pimenov. Prikladnaya matematika i informatika, **9**, 5–22 (2001). [A.G. Davydov, E.V. Zakharov, Yu.V. Pimenov. Hypersingular integral equations in computational electrodynamics. Computational Mathematics and Modeling, **14** (1), 1–15 (2003).
[124] S.I. Eminov, V.S. Eminova. ZhVMMF, **56** (3), 432–440 (2016). [S.I. Eminov, V.S. Eminova Comput. Math. Math. Phys., **56** (3), 417–425 (2016)].
[125] S.J. Obaiys, R.W. Ibrahim, A.F. Ahmad. Hypersingular Integrals in Integral Equations and Inequalities: Fundamental Review Study. In: D. Andrica, T. Rassias (eds). Differential and Integral Inequalities. Springer Optimization and Its Applications (Springer, Cham. Vol. 151, 2019. https://doi.org/10.1007/978-3-030-27407-8_25.
[126] M.V. Davidovich, A.V. Kozlov. Physics of Wave Processes and Radio Engineering Systems, **13** (2), 46–51 (2010). https://journals.eco-vector.com/pwp/article/view/53390.
[127] M.V. Davidovich, A.I. Timofeev, I.A. Kornev, V.Ya. Yavchunovskii. Izvestiya Saratovskogo universiteta Novaya Seriya. (in Russian). Seriya: Fizika **16** (1), 33–43 (2016) (in Russian)
[128] M.V. Davidovich, I.A. Kornev. Fizika volnovykh protsessov i radiotekhnicheskiye sistemy, **22** (2), 30–36 (2019) (in Russian). DOI: 10.18469/1810-3189.2019.22.2.30-36.
[129] P.G. Akishin, A.A. Sapozhnikov. Discrete and Continuous Models and Applied Computational Science, **27** (1), 60–69 (2019). DOI: 10.22363/2658-4670-2019-27-1-60-69.